Di-jets: The Path to the (un)Polarized Partonic Photon Structure at EIC

Xiaoxuan Chu

Key laboratory of Quark & Lepton Physics Institute of Particle Physics

Brookhaven National Lab

DIS 2018, 16-20 April
Kobe, Japan

Outline

- **Introduction**
- **Jets at EIC**
  - q/g jet discrimination
  - Underlying events
- **Photon structure at EIC**
  - Unpolarized photon PDFs
  - Flavor tagging
  - Polarized photon PDFs
- **Summary**

Part 1
Jets at EIC

Why jets?

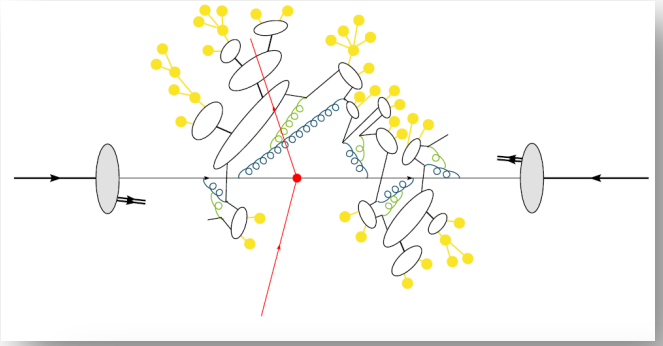

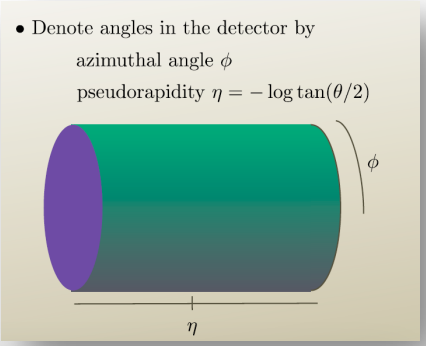

- Partons produced in hard scattering
- Parton radiation
- Hadronization

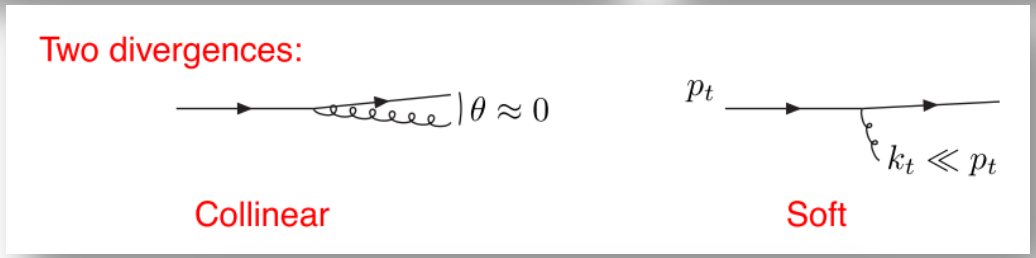

- High possibility to get a spray of collimated particles with high momentum
- And also low momentum particle under wide angles

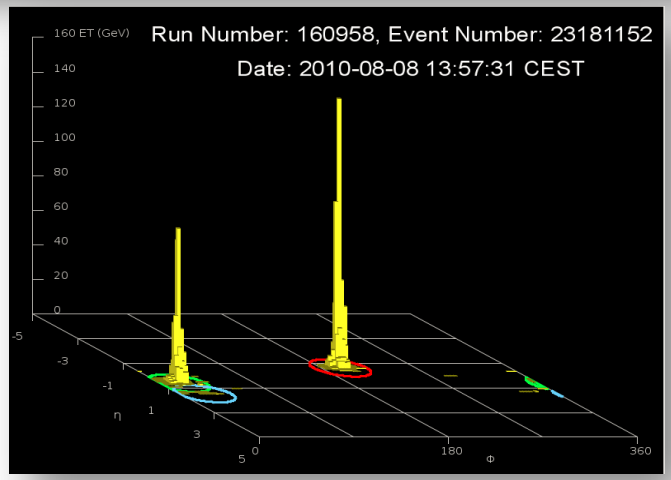

- The evidence of di-jet: two sprays of particles are detected.
- Jets carry more information on the original partons than hadrons

Di-jets at EIC from PYTHIA

Resolved

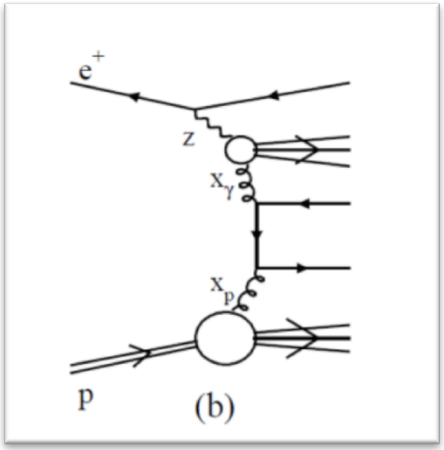

Direct

Photon-Gluon Fusion & QCD-Compton

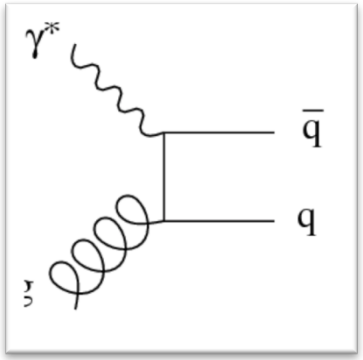

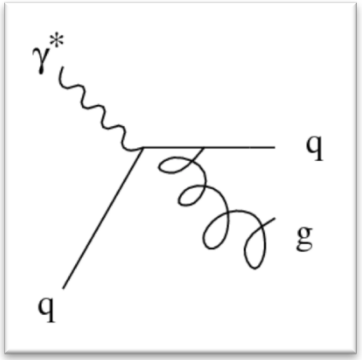

- **PYTHIA** is used in the event generation. FastJet is used for jet reconstruction.
- **Anti-k_T algorithm** is applied.
- Di-jet events are selected by the cuts: trigger jet and associate jet p_T>4.5 GeV.
- Do **geometry matching** in the simulation, we can tag quark/gluon jets.

$$\Delta R\{parton - jet\} = \sqrt{\Delta\phi^2 + \Delta\eta^2}$$

q/g jet discrimination

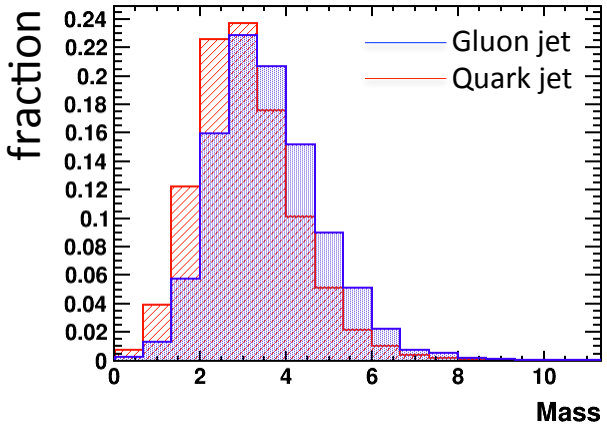

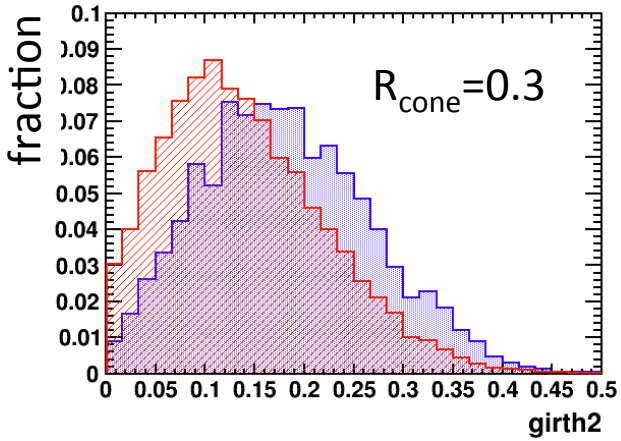

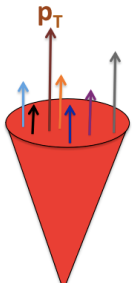

Leading hadron p_T fraction

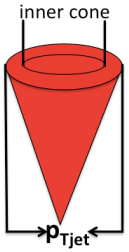

$$girth2 = \sum_{i \in jet} \frac{p_T^i}{p_T^{jet}} |R_i|^2$$

$$profile = \sum_{i \in cone} \frac{p_T^i}{p_T^{jet}}$$

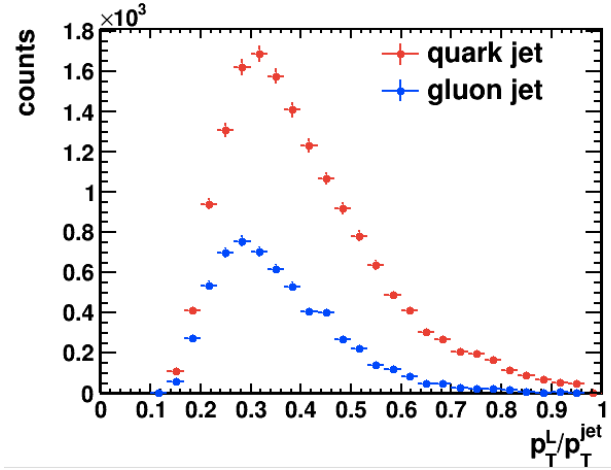

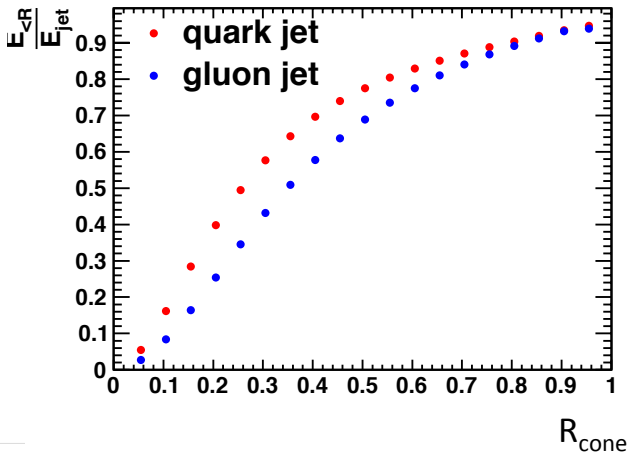

1. Gluon jet mass is a little higher than quark jet one.
2. The p_T of leading hadron is higher in quark jet than in gluon jet.
3. Quark jet is more collimated than gluon jet.

TMVA Method

Plots are from Brian Page:

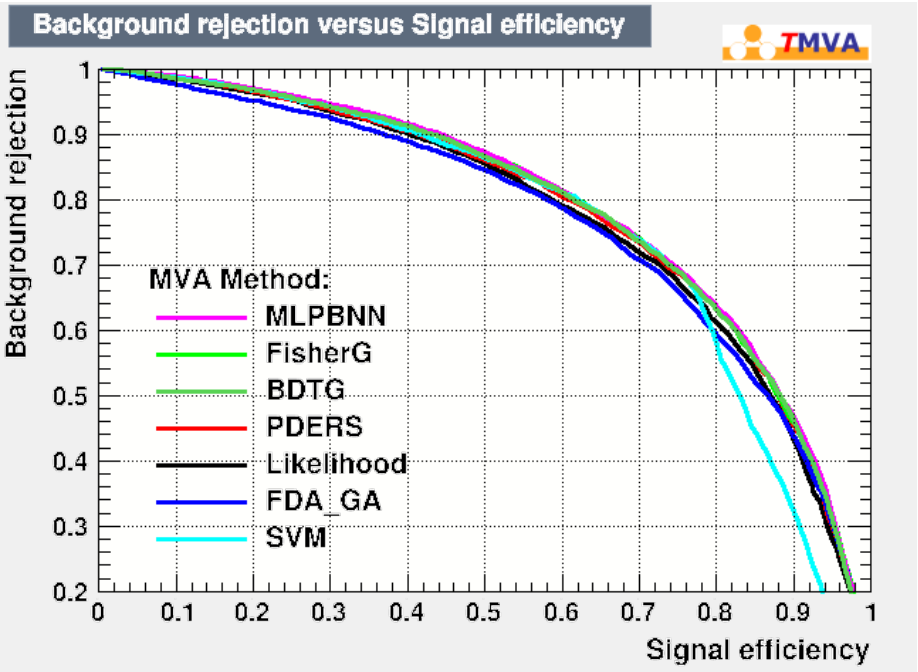

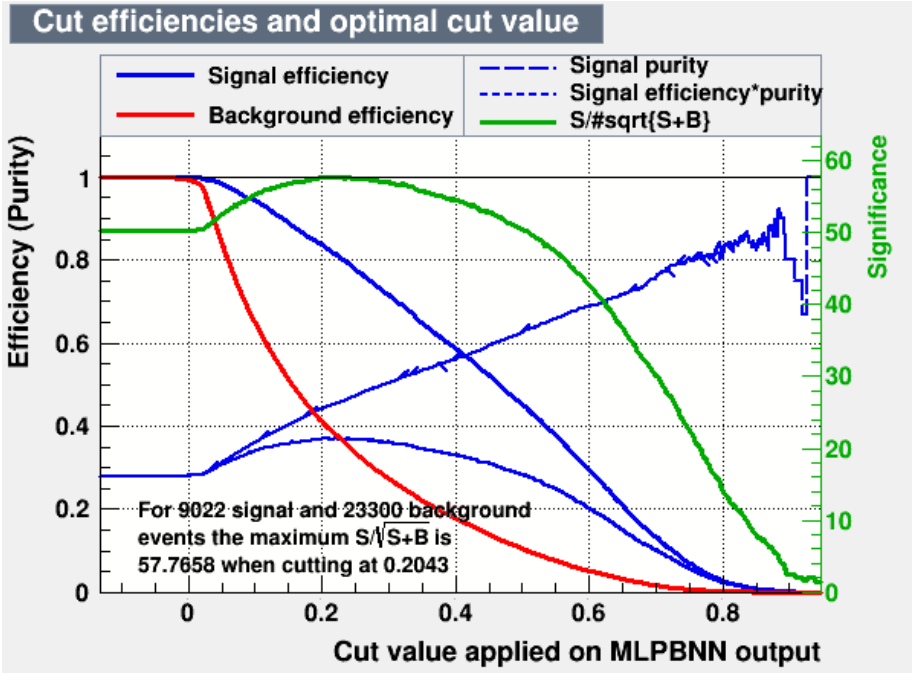

Toolkit for Multivariate Data Analysis with ROOT(TMVA)
For current study, place cut where signal purity = signal efficiency

Underlying events (region method)

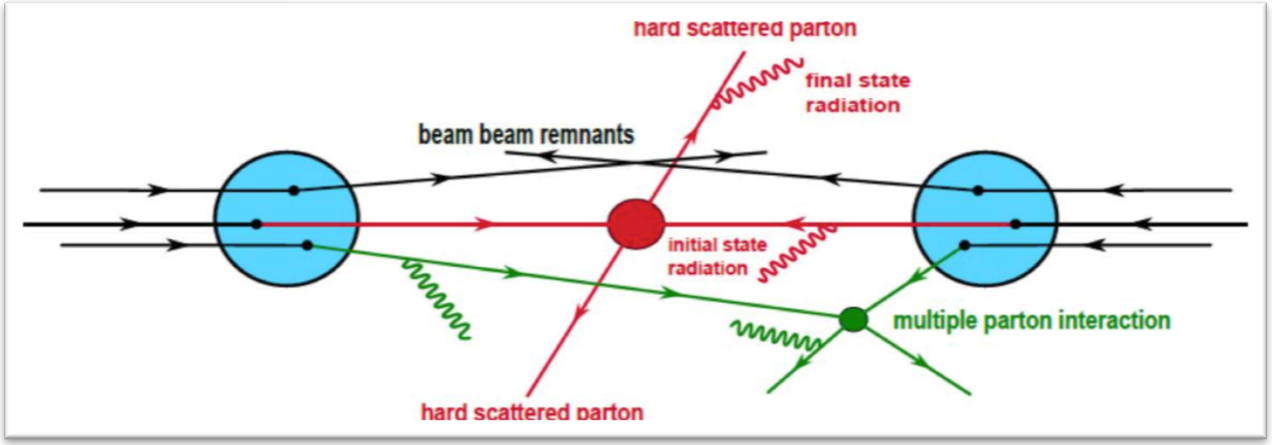

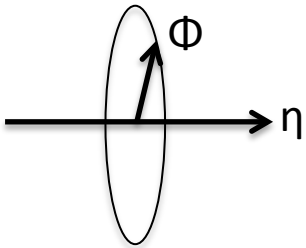

Underlying events: everything except the particles fragmented from the hard scatted partons

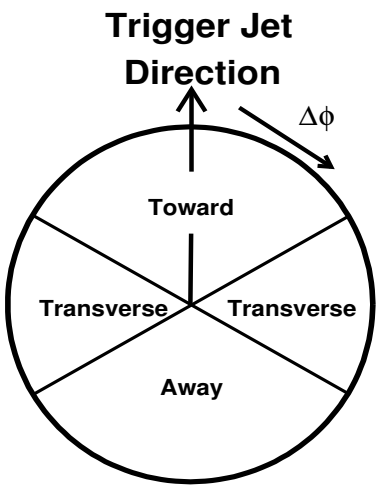

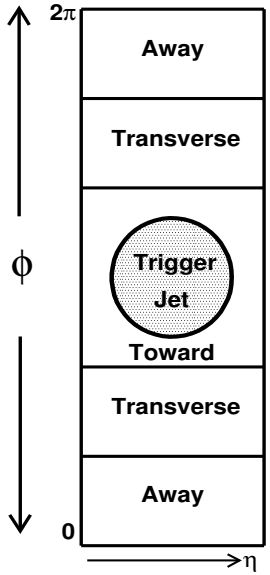

Toward: $|\Delta\Phi| < 60$ degree,
Transverse: $60<|\Delta\Phi| < 120$,
Away: $|\Delta\Phi| >120$

Trigger Jet is Jet with highest p_T
$\Delta\Phi = \Phi\_part - \Phi\_Jet1$

Measurements:
1. charged multiplicity density, sum pt density
2. Density difference in 3 regions

Underlying events

Charged particle multiplicity density

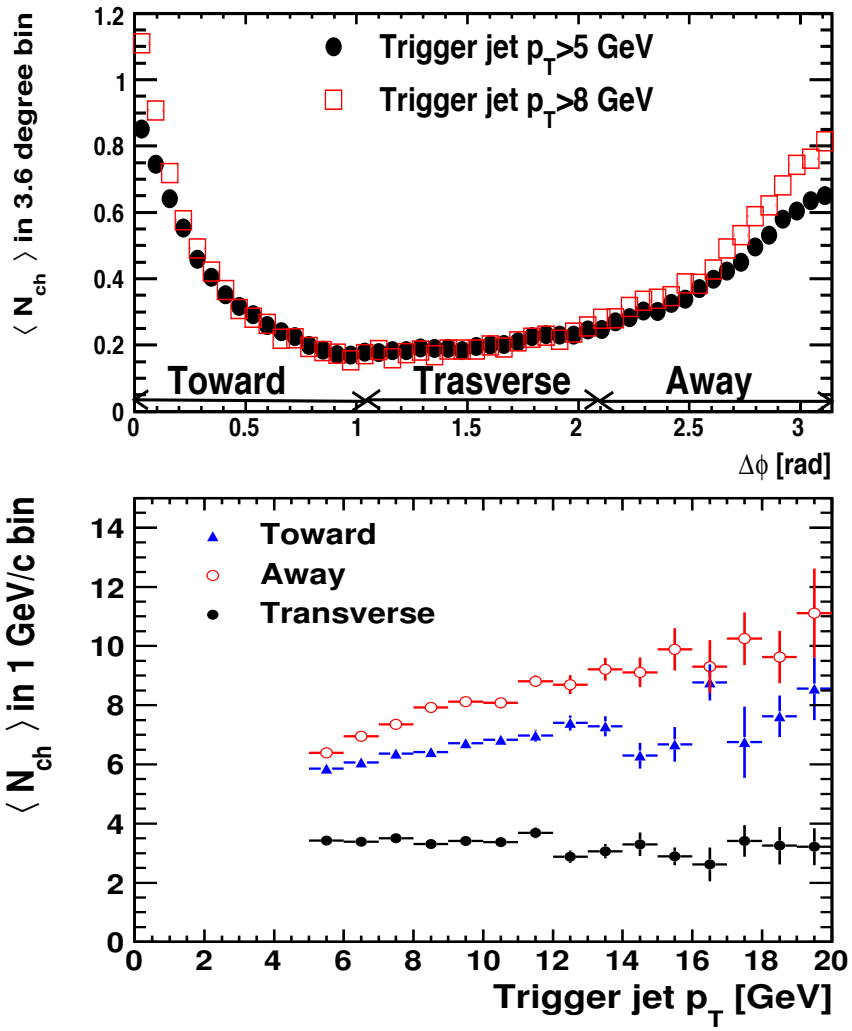

Energy density

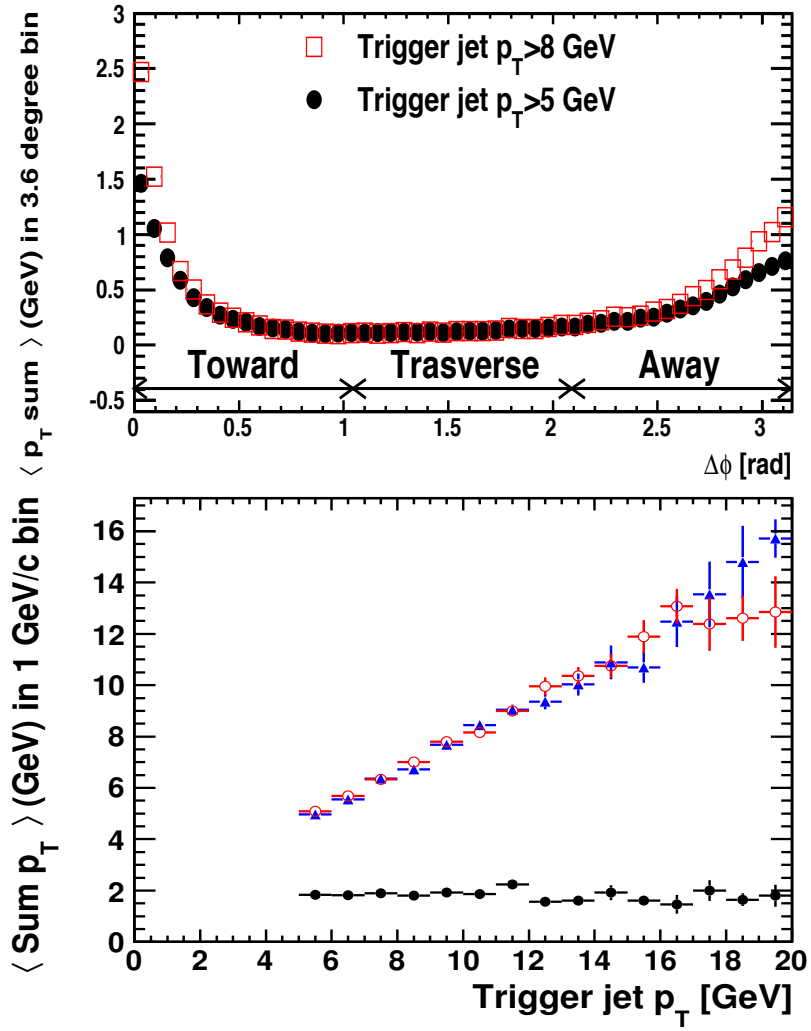

off-axis method

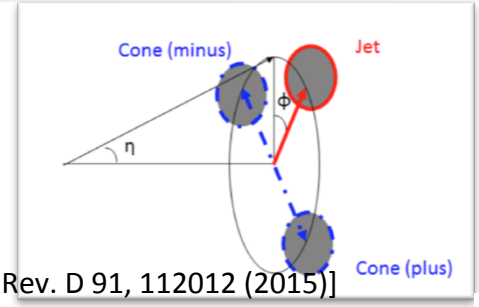

[Phys. Rev. D 91, 112012 (2015)]

- ✓ In each event, we analyze jets with high momentum, jet by jet.
- ✓ For each jet, we define two cones (r = 0.4).
- ✓ Each cone is centered at the same as the jet but ±π/2 away in Φ from the jet Φ.
- ✓ Take the particles from the two cones as underlying event.

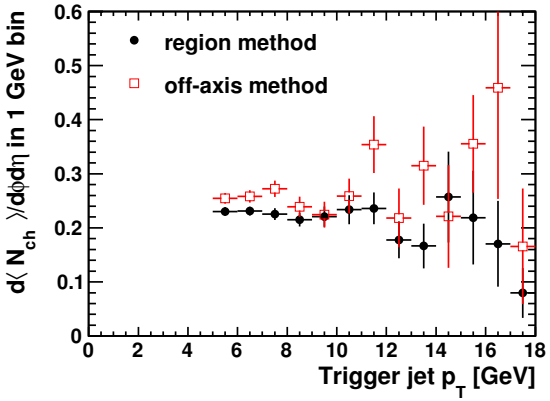

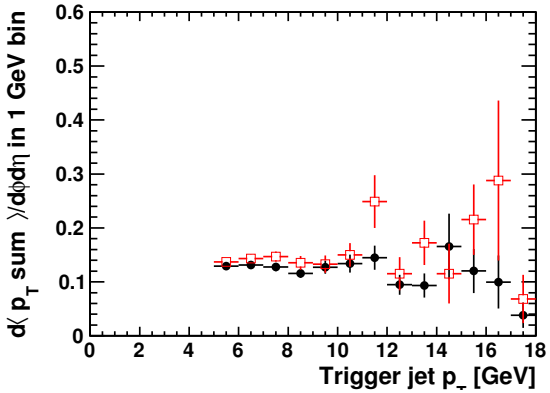

Results from the two different methods are consistent.

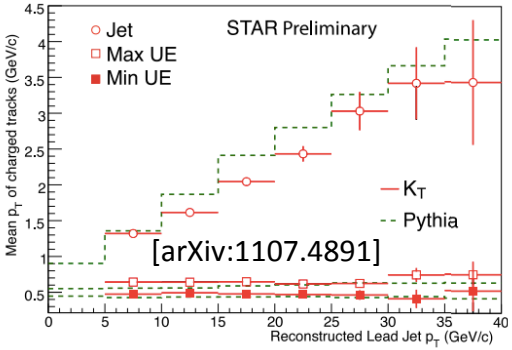

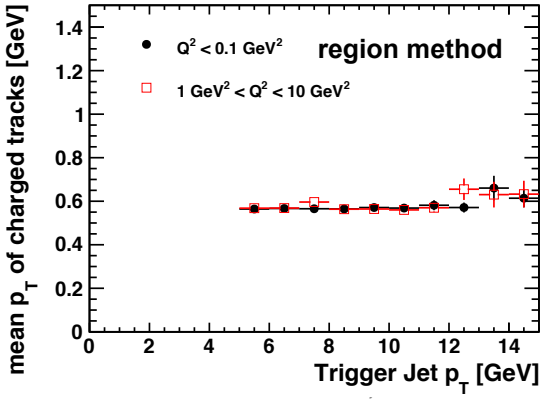

Compared with data from STAR.

Zilong Chang's talk tomorrow.

Part 2
Photon structure @ EIC

Di-jet in resolved/direct process

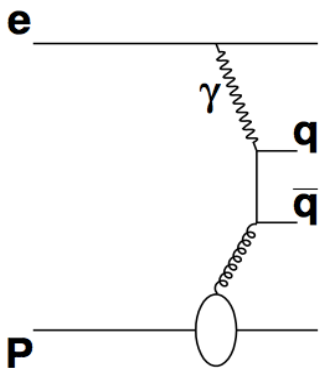

PGF: Di-jet produced

"Direct process"

- Point-like photon (no substructure)
- x_γ is equal to 1

"Resolved process"

- Hadronic photon (with strcture)
- x_γ is smaller than 1
- Di-jet production

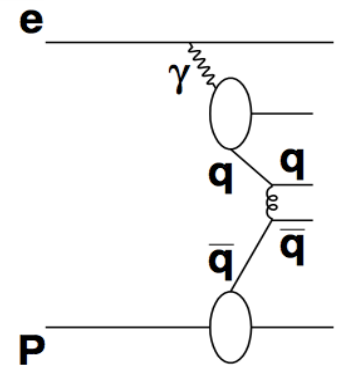

Similar with pp collision

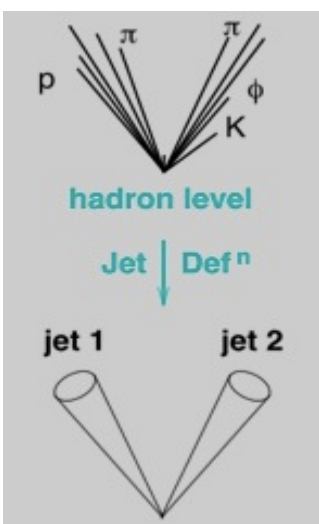

- **Separate di-jet produced in resolved and direct processes**, to get clear resolved process
- Reconstruct x_γ by using di-jet as observables: $x_\gamma^{rec} = \frac{1}{2E_e y}(p_{T1}e^{-\eta_1} + p_{T2}e^{-\eta_2})$
  - Two jets with highest p_T
  - Parton densities in the photon can be extracted by measuring **di-jet cross section**

$$\frac{d^2\sigma}{dx_\gamma dp_T} = \gamma_{flux} \otimes PDF_\gamma(x_\gamma, Q^2, \mu) \otimes PDF_p(x_p, \mu) \otimes d\sigma_{ij}(\theta^*, Q^2, \mu)$$

Reproduce HERA data

Kinematics cuts from HERA:

27.5GeV×820GeV, 0.2<y<0.83,

$|\Delta\eta^{jets}|<1$, $0<\eta^{jet1}+\eta^{jet2}<4$

E^{jet1}_T, E^{jet2}_T>7.5 GeV ,

$E^{jet1}_T+E^{jet2}_T$>20GeV,

$|E^{jet1}_T-E^{jet2}_T|/(E^{jet1}_T+E^{jet2}_T)<0.25$

Strong correlation observed between x^{rec}_γ and the input x^{input}_γ in the simulation indicates **the di-jet observable** is ideal to reconstruct x_γ

Reconstruction provides a good way to **separate direct/resolved** x^{rec}_γ contribution(x^{rec}_γ < 0.75)

Our simulation results produce the existing data well

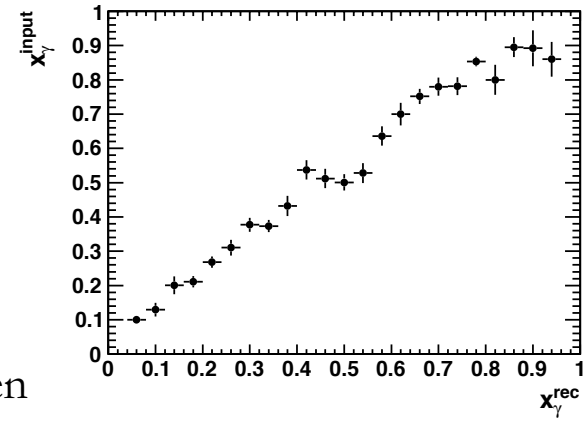

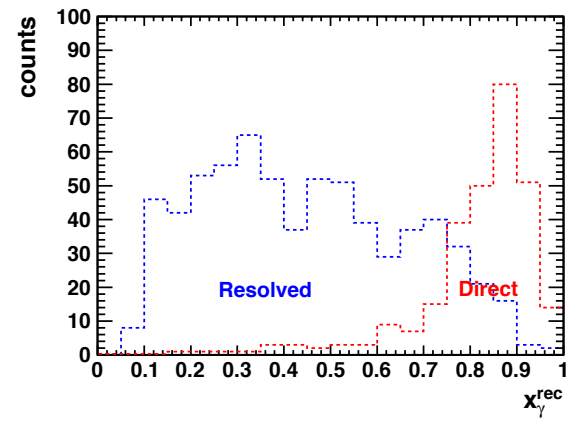

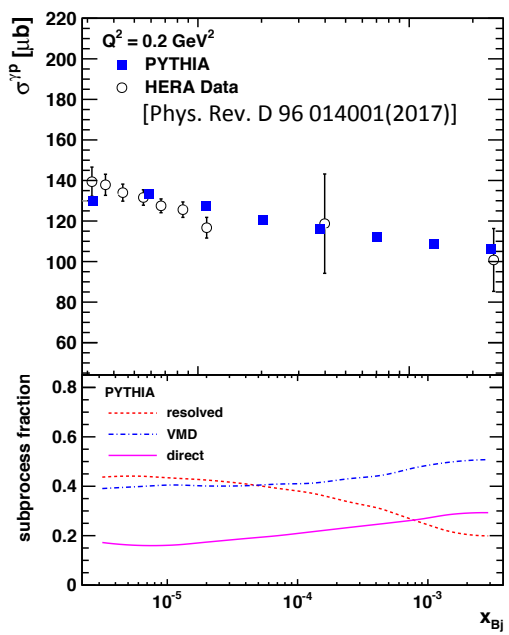

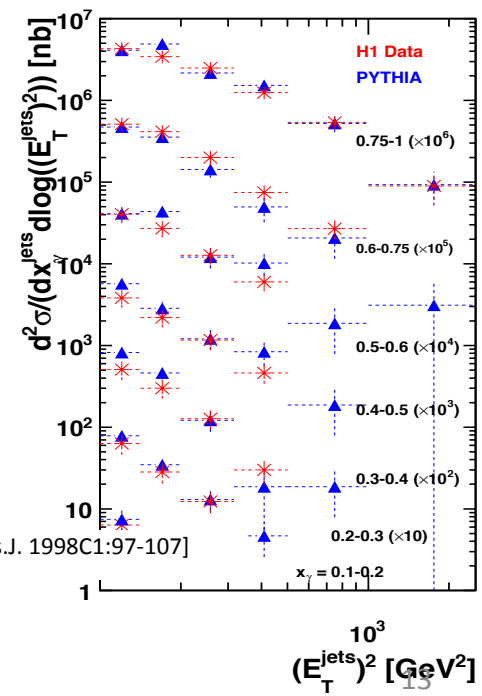

[Eur.Phys.J. 1998C1:97-107]

Unpolarized photon structure @ EIC

20GeV×250GeV, 0.01<y<0.95, two highest p_T jets, , p^{jet1}_T>5 GeV, p^{jet1}_T>p^{jet2}_T>4.5 GeV, $|\eta^{jets}|$<4.5, Inside the jet, stable particle p_T>250MeV

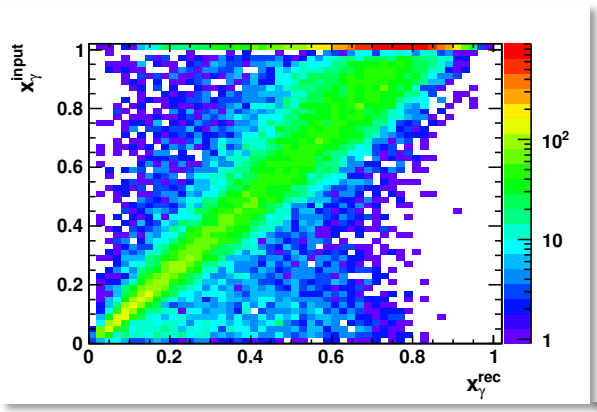

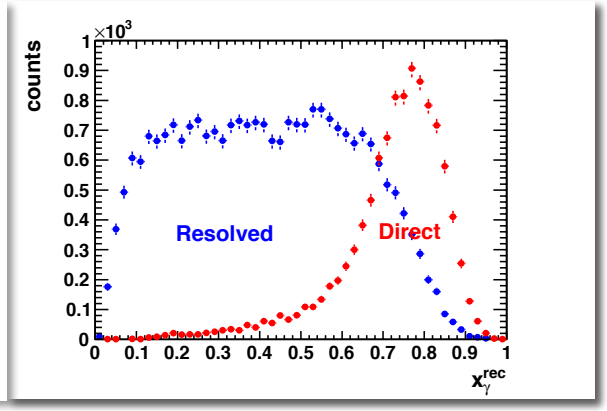

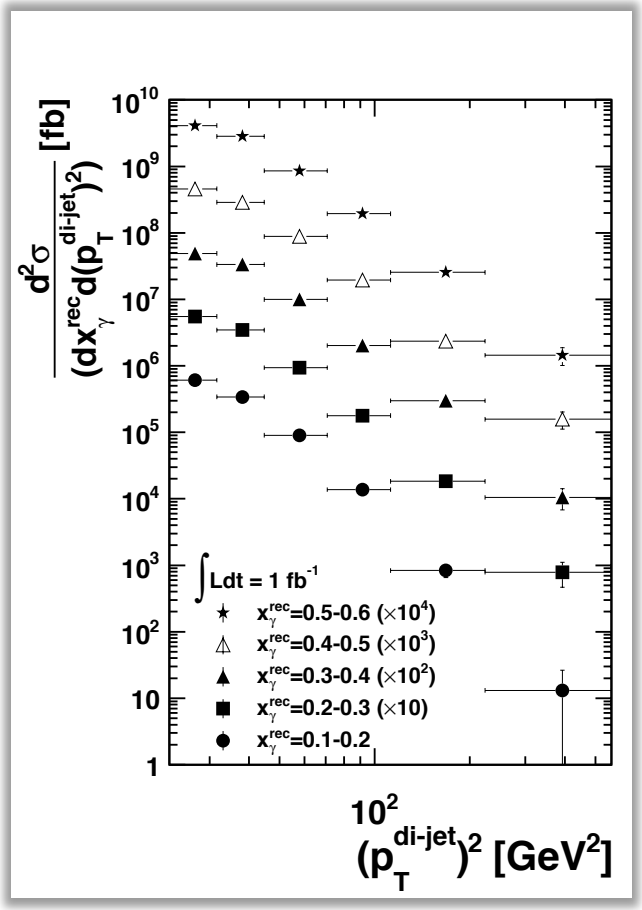

- Di-jet method provides a good way to reconstruct x^{rec}_γ
- Di-jet method can help us separate resolved/direct process (x^{rec}_γ< 0.6)
- The simulation shows the capability to measure the cross section for di-jet production, with high accuracy in a wide kinematic range at EIC and extract the unpolarized photon PDFs from a global fit

Select jet from the photon side

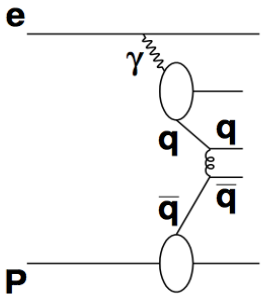

Separate jets from photon side and proton side

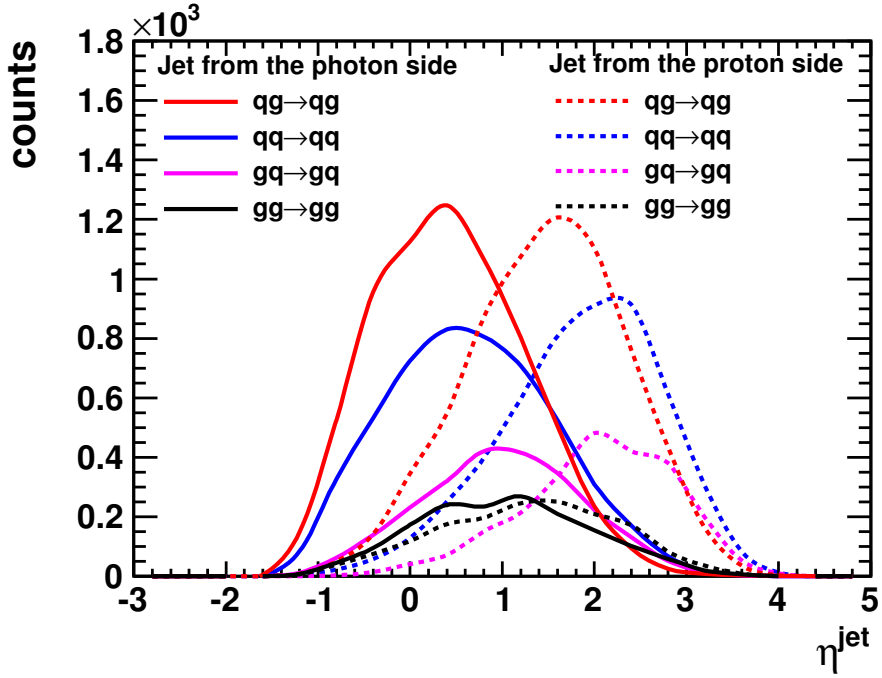

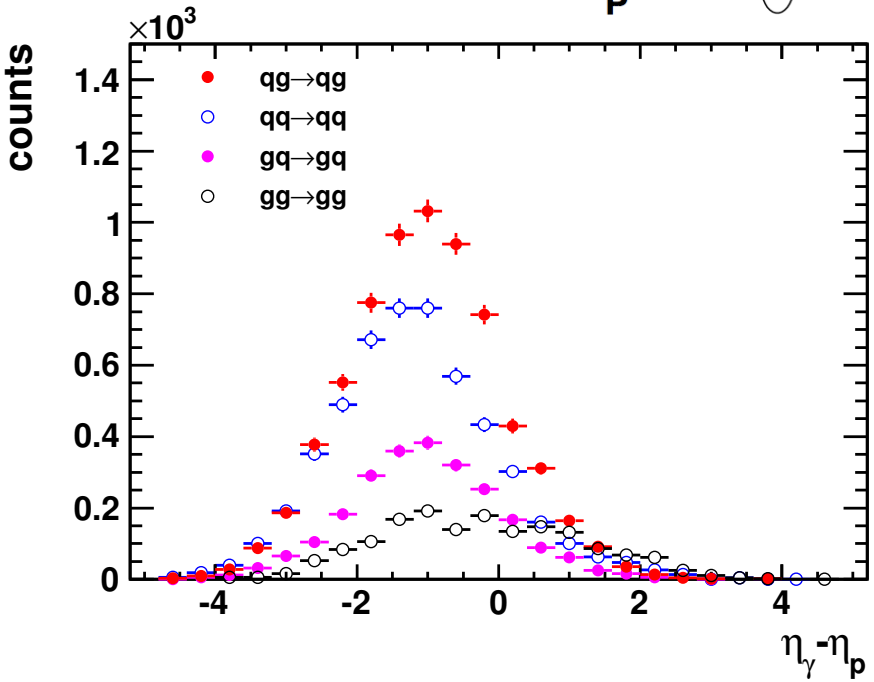

- Jet from the photon side dominates at more negative pseudo-rapidity region
- ~82% of delta pseudo-rapidity < 0

Flavor tagging: quarks

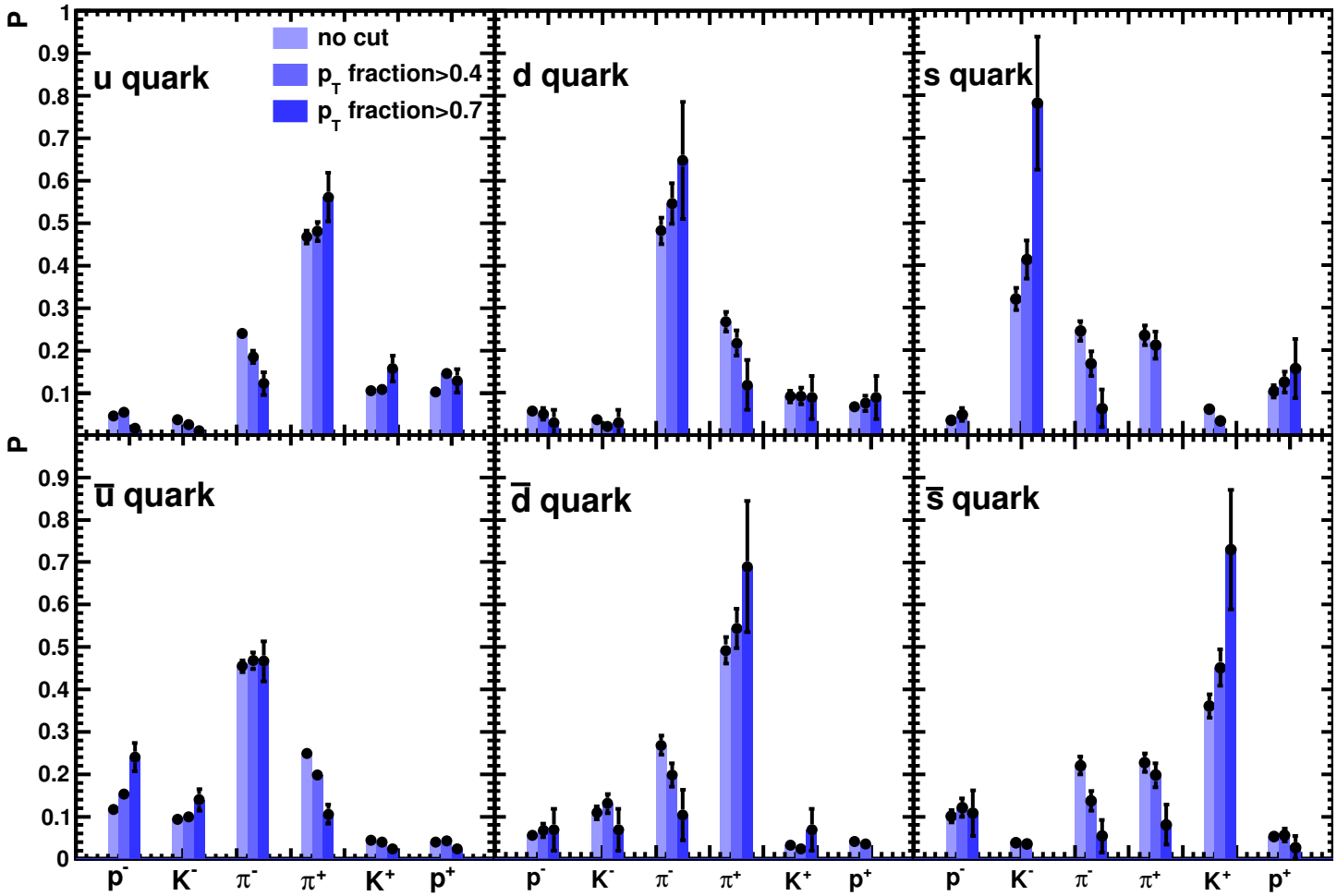

Polarized cross section

$$\frac{d^2\Delta\sigma}{dx_\gamma dp_T} = \gamma_{flux} \otimes \Delta PDF_\gamma(x_\gamma, Q^2, \mu) \otimes \Delta PDF_p(x_p, \mu) \otimes d\sigma_{ij}(\theta^*, Q^2, \mu)$$

$$\Delta\sigma = \frac{1}{2}(\sigma^{++} - \sigma^{+-})$$

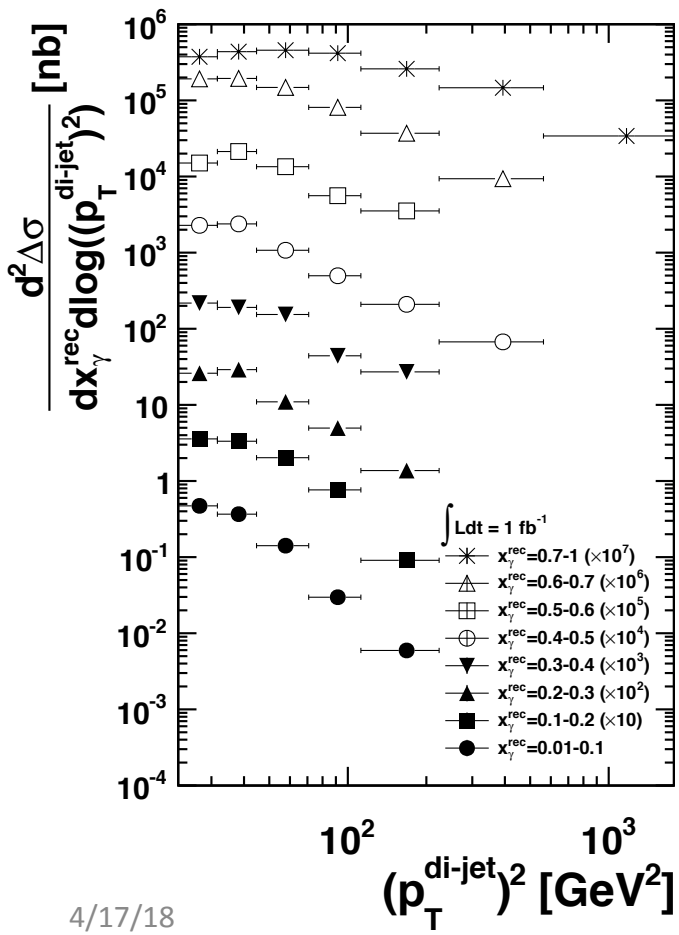

- The simulation shows the capability to measure the polarized cross section for di-jet production, with high accuracy in a wide kinematic range at EIC
- First measurement of polarized photon PDFs with high precision
- Flavor tagging can also be applied in polarized case

Input: polarized proton-PDF: DSSV-14
photon-PDF: Phys. Lett. B 337 373-375 (1994)

Asymmetry

$$A_{LL} = \Delta\sigma / \sigma$$

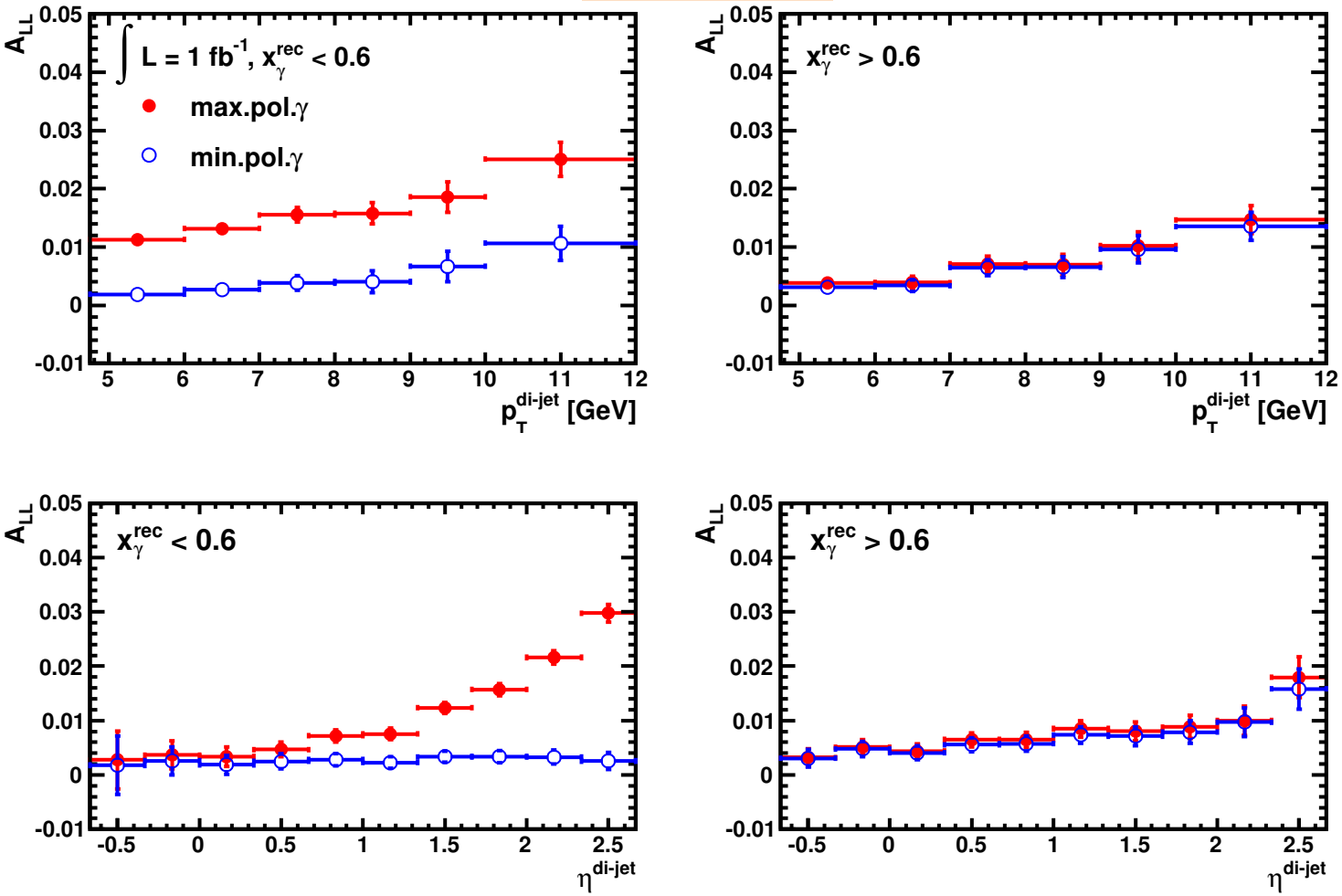

Input: polarized proton-PDF: DSSV-14 photon-PDF: Phys. Lett. B 337 373-375 (1994)

Advantages @ EIC

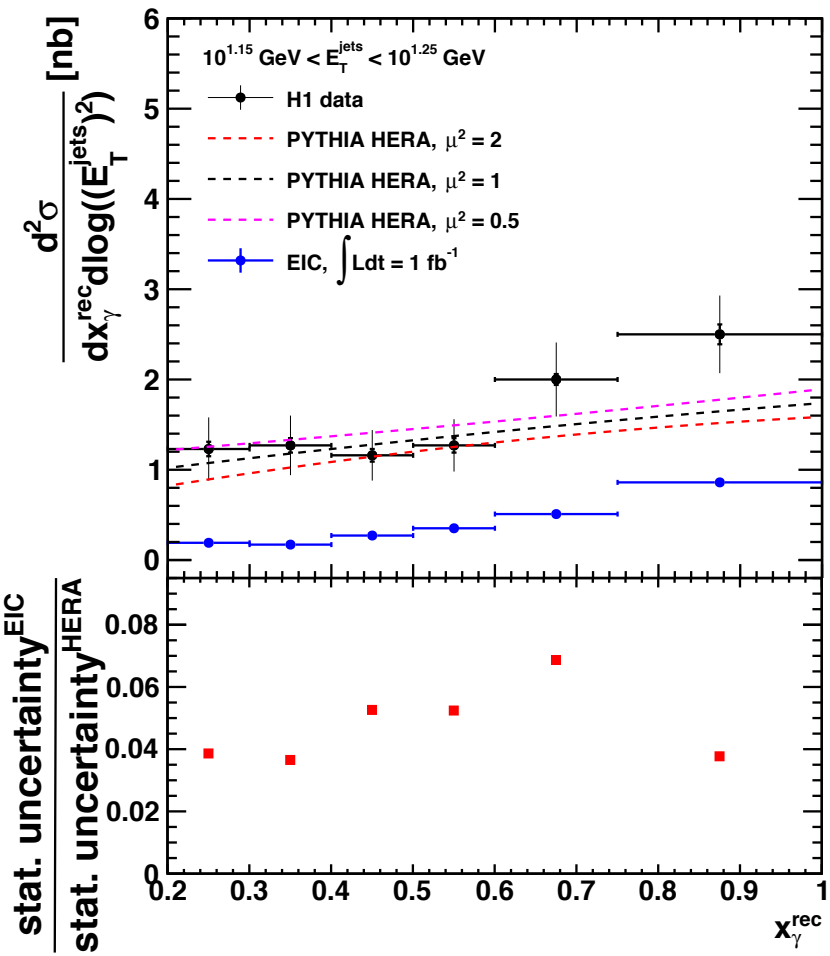

- High luminosity to define the uncertainty band
- First measurement of polarized photon PDFs with high precision
- Flavor tagging can also be applied in polarized case

Summary

- **Jets are reconstructed @ EIC**
  - Quark jet and gluon jet discrimination
  - Underlying events
- **Photon PDFs can be extracted by reconstructing x_γ**
  - x^{rec}_γ is correlated with input
  - We can effectively access the underlying photon PDFs at EIC
- **Flavor tagging can be applied to identify the flavor of the parton from the photon**
- **Pol. Photon PDF can the first time be measured in the world.**

[Ref:Phys.Rev.D.96.074035]

Back up

Planed EIC @ BNL: eRHIC

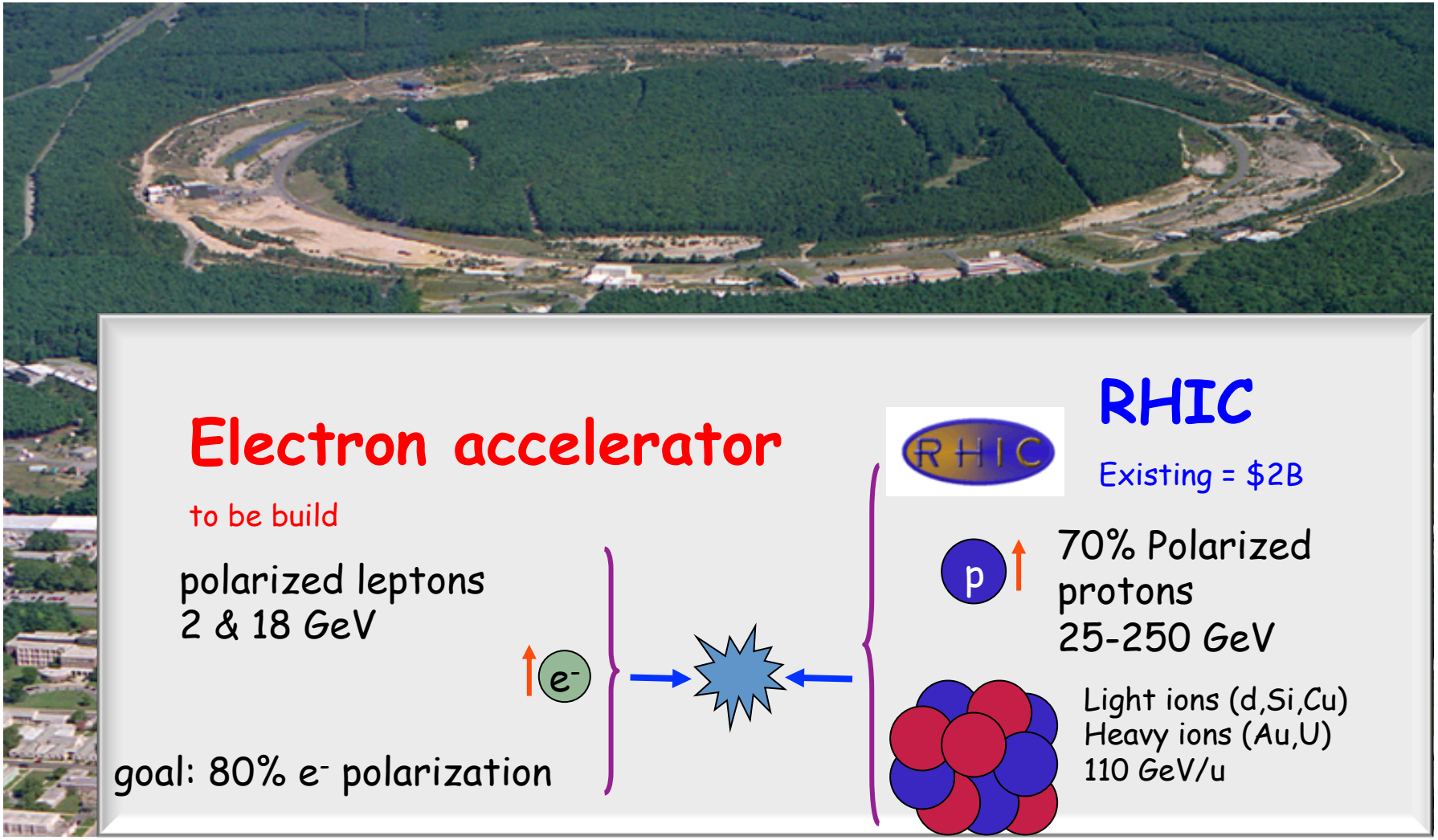

Use simulation to reproduce data

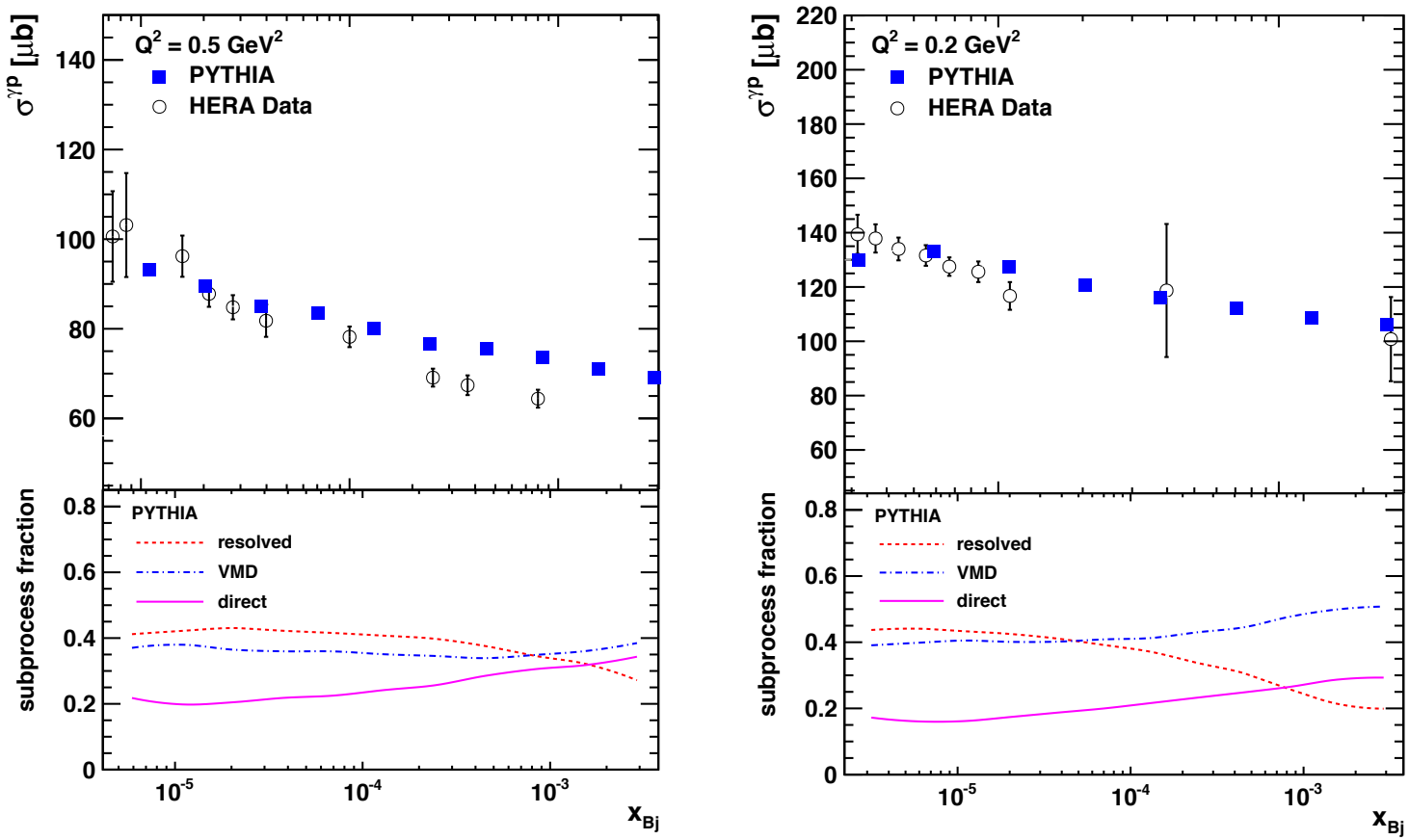

- **PYTHIA** is used in simulation to generate each event : all particle info during the whole collision process, we reproduce the world data, the simulation is reliable.

Proton partonic kinematics

Parton momentum fraction: photon gluon fusion

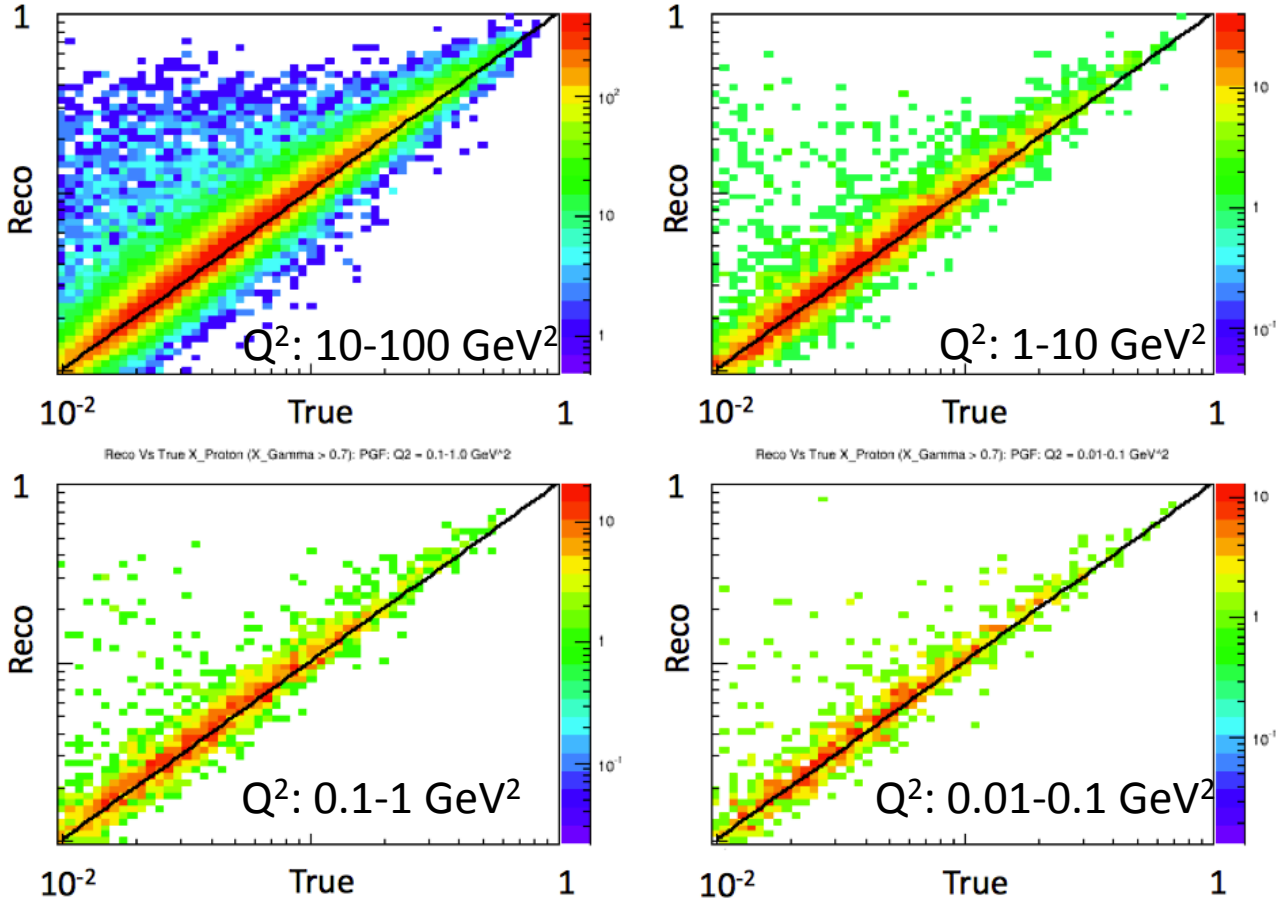

- To measure gluon, need to probe the parton coming from the proton
- Momentum fraction of the parton from proton is well reconstructed

$$x_p^{rec} = \frac{1}{2E_p}(p_{T1}e^{\eta_1} + p_{T2}e^{\eta_2})$$

Direct Vs resolved process

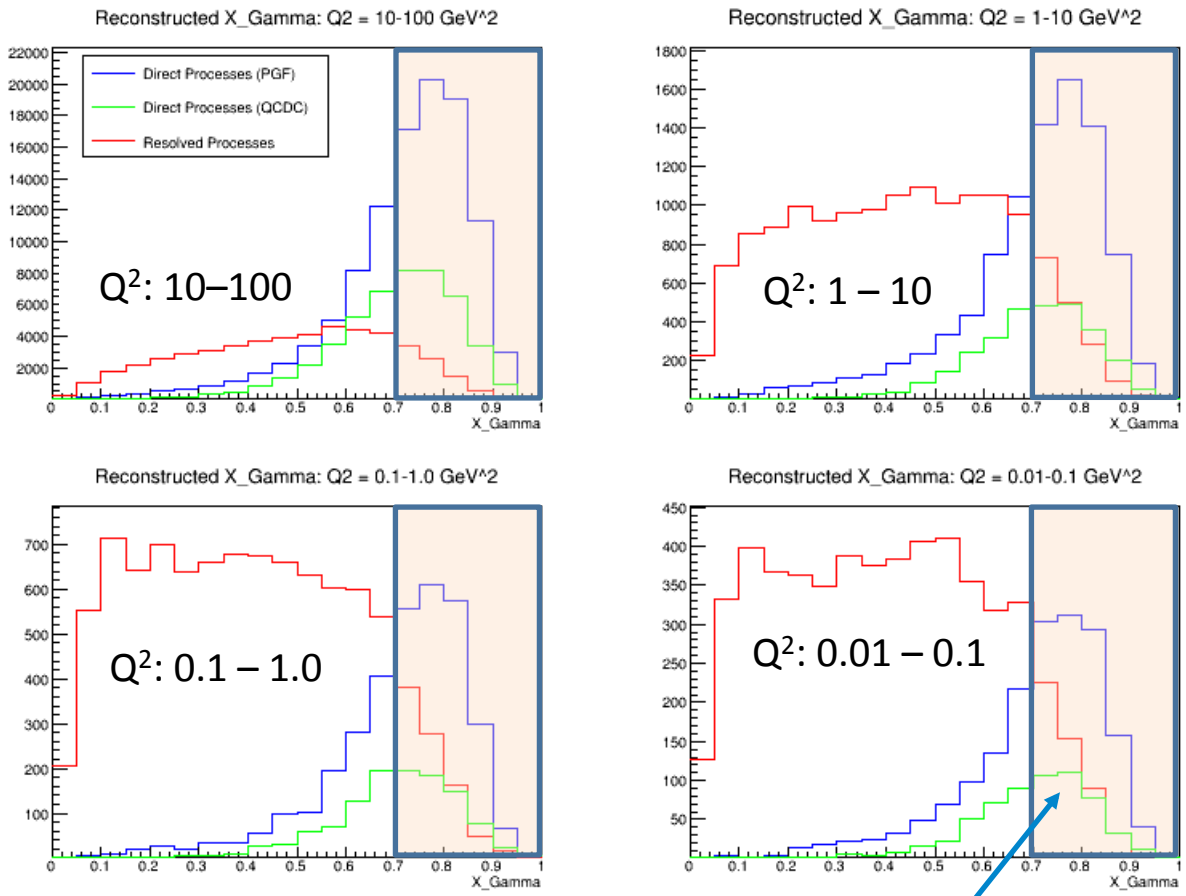

$$x_\gamma^{rec} = \frac{1}{2E_e y}(p_{T1}e^{-\eta_1} + p_{T2}e^{-\eta_2})$$

Accepted Region

- Plot reconstructed X_γ for direct and resolved processes
- Direct processes should concentrate toward 1 while resolved processes are at lower values
- Direct processes dominate at higher Q^2 while resolved are more prevalent at low Q^2
- Cut of $X_\gamma > 0.7$ enhances the direct fraction at all Q^2

PYTHIA simulation

$$w = \hat{a}(\hat{s},\hat{t},\mu^2,Q^2) \bullet \frac{\Delta f_a^{\gamma^*}(x_a,\mu^2)}{f_a^{\gamma^*}(x_a,\mu^2)} \bullet \frac{\Delta f_b^{N}(x_b,\mu^2)}{f_b^{N}(x_b,\mu^2)}$$

PYTHIA Input Set	
Q^2	10^{-5} - 1
Proton PDFs	CTEQ 5M
Photon PDFs	SAS

Polarized photon PDF(delta f_a)	
Minimal polarization	$\Delta f_a^{\gamma^*}(x_a,\mu^2) = 0$
Maximal polarization	$\Delta f_a^{\gamma^*}(x_a,\mu^2) = f_a^{\gamma^*}(x_a,\mu^2)$
Polarized proton PDF(delta f_b)	**DSSV**

UnPolarized photon PDF(f_a)	CTEQ 5m
UnPolarized proton PDF(f_b)	SAS

Flavor tagging: quarks

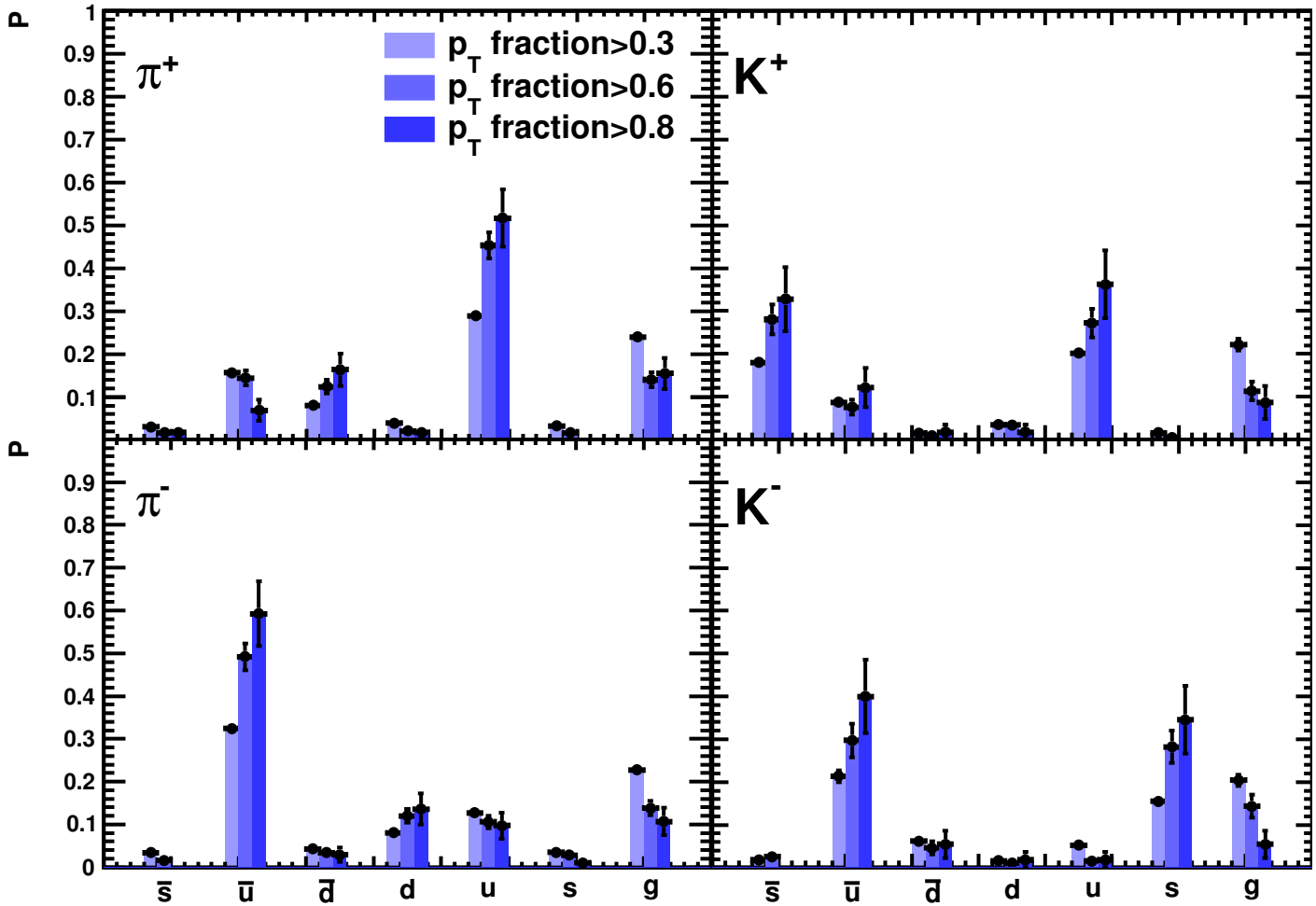

EIC: Polarized ep collider

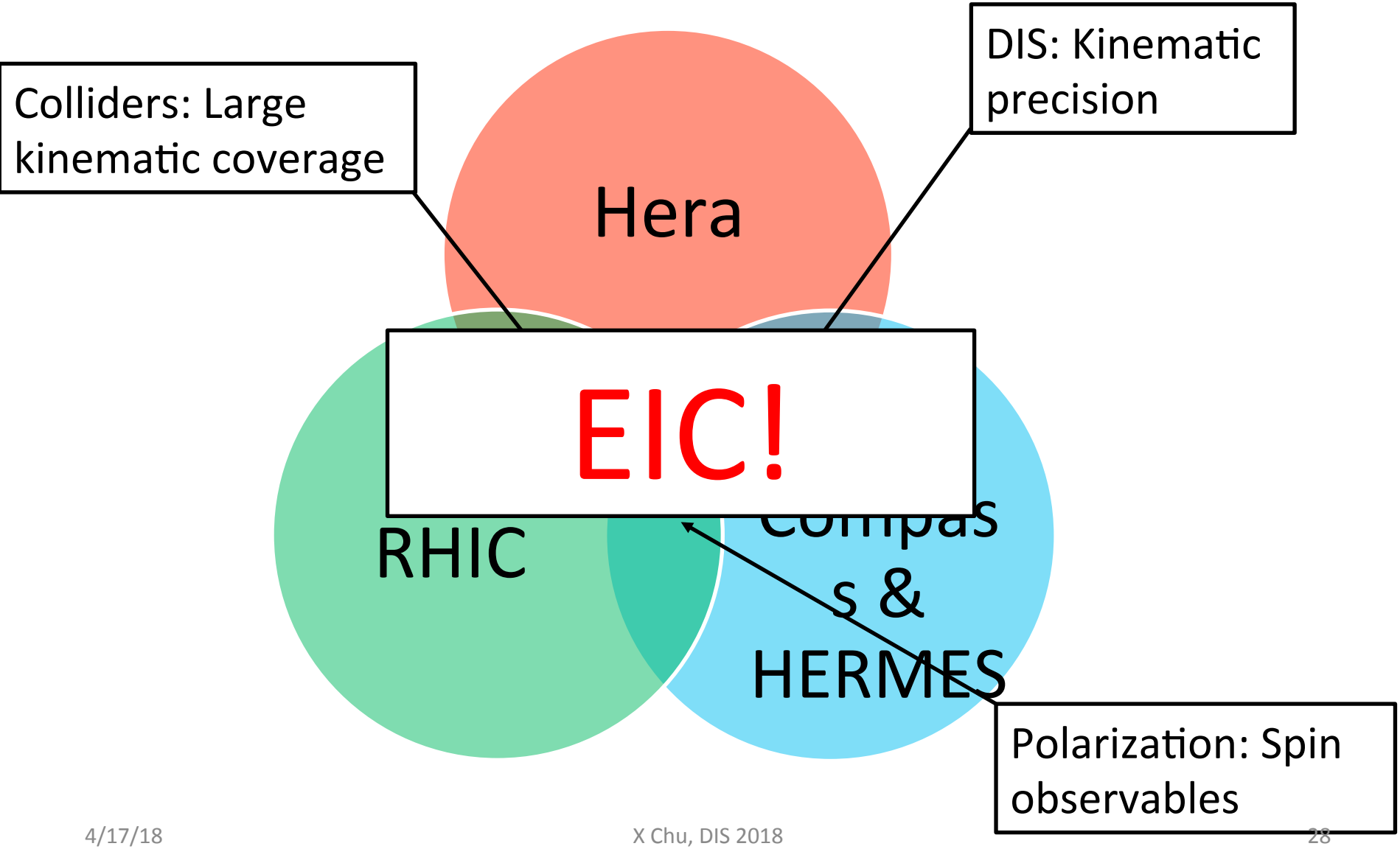

Motivation

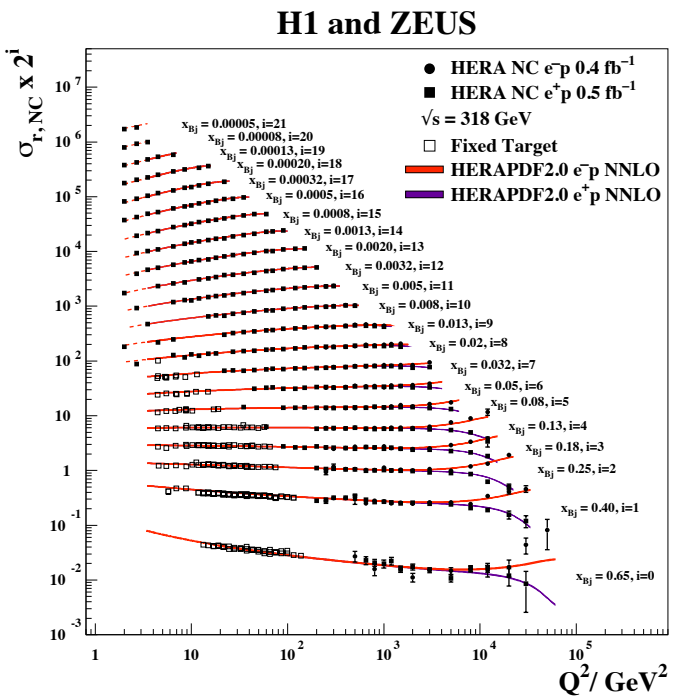

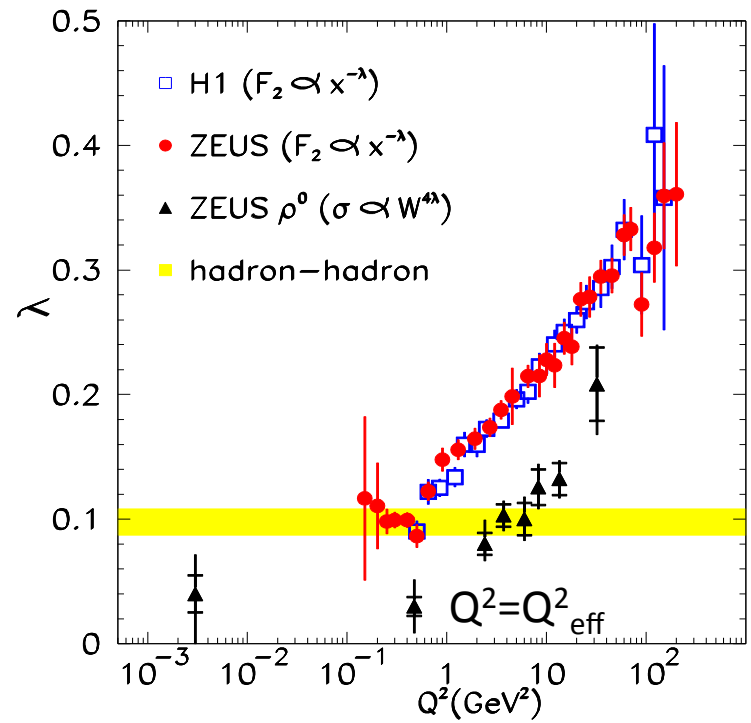

$$\frac{d^2\sigma^{NC}_{e^{\mp}p}}{dxdQ^2} = \frac{2\pi\alpha^2_{em}Y_+}{xQ^4}\left(F_2 - \frac{y^2}{Y_+}F_L \pm \frac{Y_-}{Y_+}xF_3\right)$$

$q(x,Q^2) - \bar{q}(x,Q^2)$ $\quad g(x,Q^2)$ $\quad q(x,Q^2) + \bar{q}(x,Q^2)$

- Does the kink occur at the same Q^2 for eA and for polarized ep
- Photon structure as fct. of Q^2

Kinematics cuts for di-jet methods

20GeV×250GeV, 0.01<y<0.95, two highest p_T jets, , p^{jet1}_T>5 GeV, p^{jet1}_T>p^{jet2}_T>4.5 GeV, $|\eta^{jets}|$<4.5, Inside the jet, stable particle p_T>250MeV

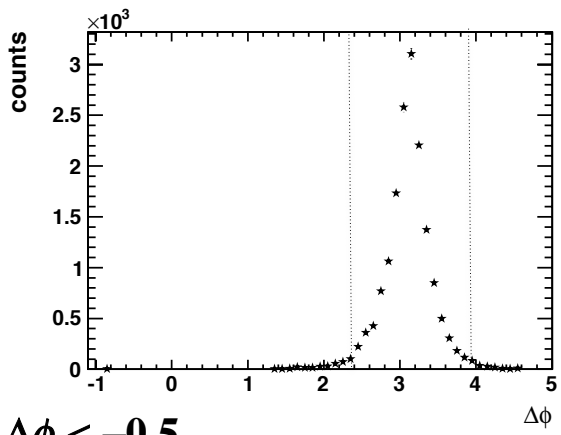

$\cos\Delta\phi < -0.5$

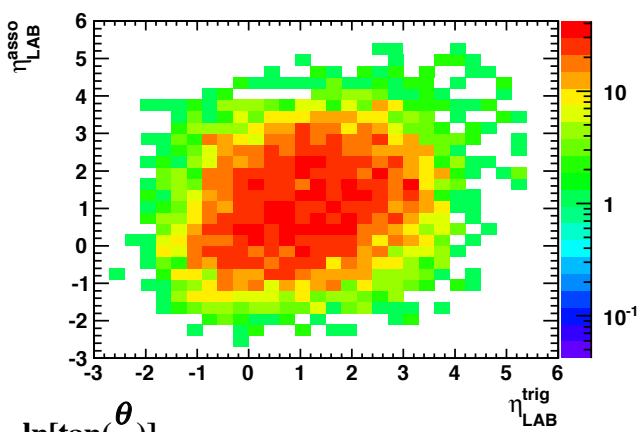

$\eta \equiv -\ln[\tan(\frac{\theta}{2})]$

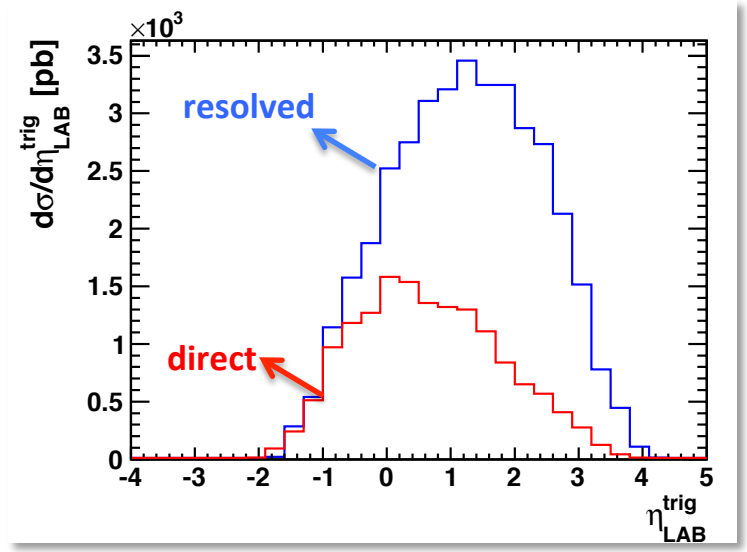

- At positive η_{LAB} , especially $\eta_{LAB} > 2$, the cross section is dominated by resolved process
- $\eta^{asso}{}_{LAB}$ distribution of associate jet shows the same result

Same method of probing the photon structure

Probe the proton structure

Accessing proton with di-jets

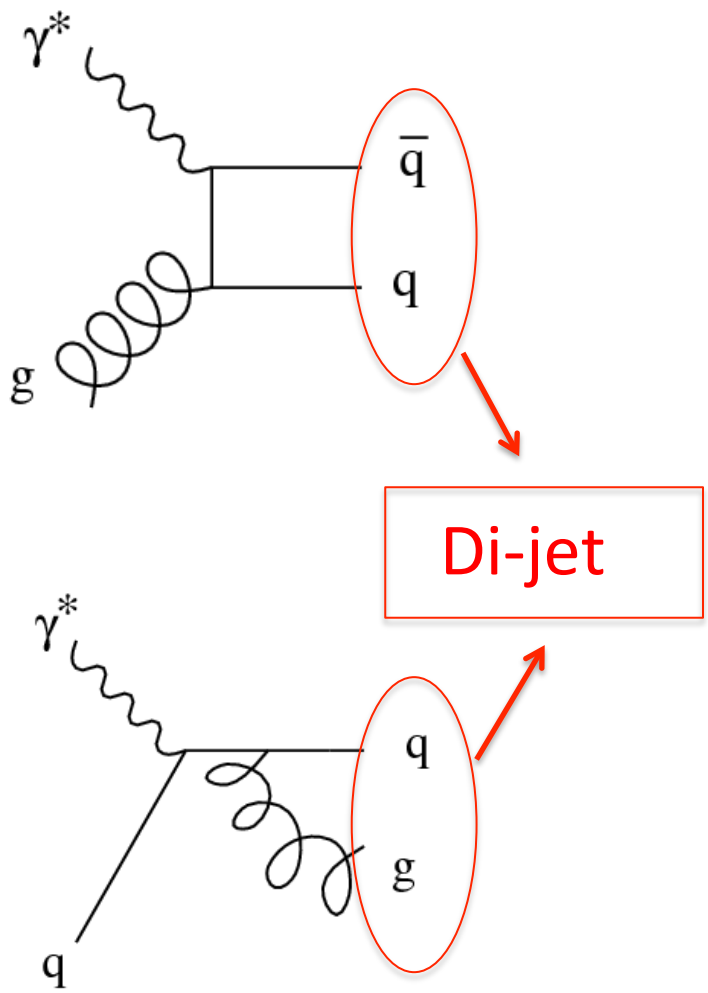

- Gluons can be probed in DIS via the higher-order photon gluon fusion process
- Also have the QCD – Compton process which probes quarks at the same order
- Both processes produce 2 angularly separated hard partons -> Di-jet
- At lower Q2, resolved processes in which the photon assumes a hadronic structure begin to dominate, interested in the parton from the proton, would like to suppress the resolved component

Direct Vs resolved process

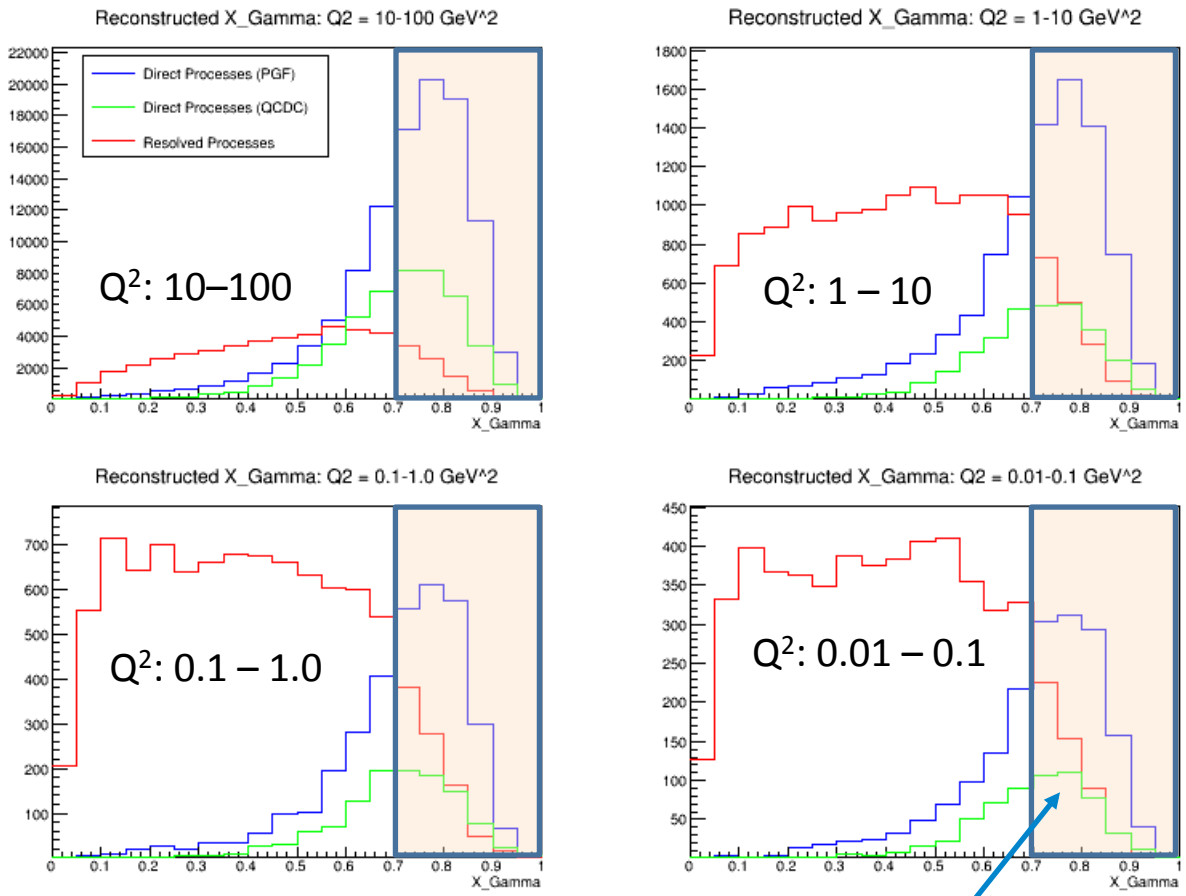

$$x_\gamma^{rec} = \frac{1}{2E_e y}(p_{T1}e^{-\eta_1} + p_{T2}e^{-\eta_2})$$

Accepted Region

- Plot reconstructed X_γ for direct and resolved processes
- Direct processes should concentrate toward 1 while resolved processes are at lower values
- Direct processes dominate at higher Q^2 while resolved are more prevalent at low Q^2
- Cut of $X_\gamma > 0.7$ enhances the direct fraction at all Q^2

Proton partonic kinematics

Parton momentum fraction: photon gluon fusion

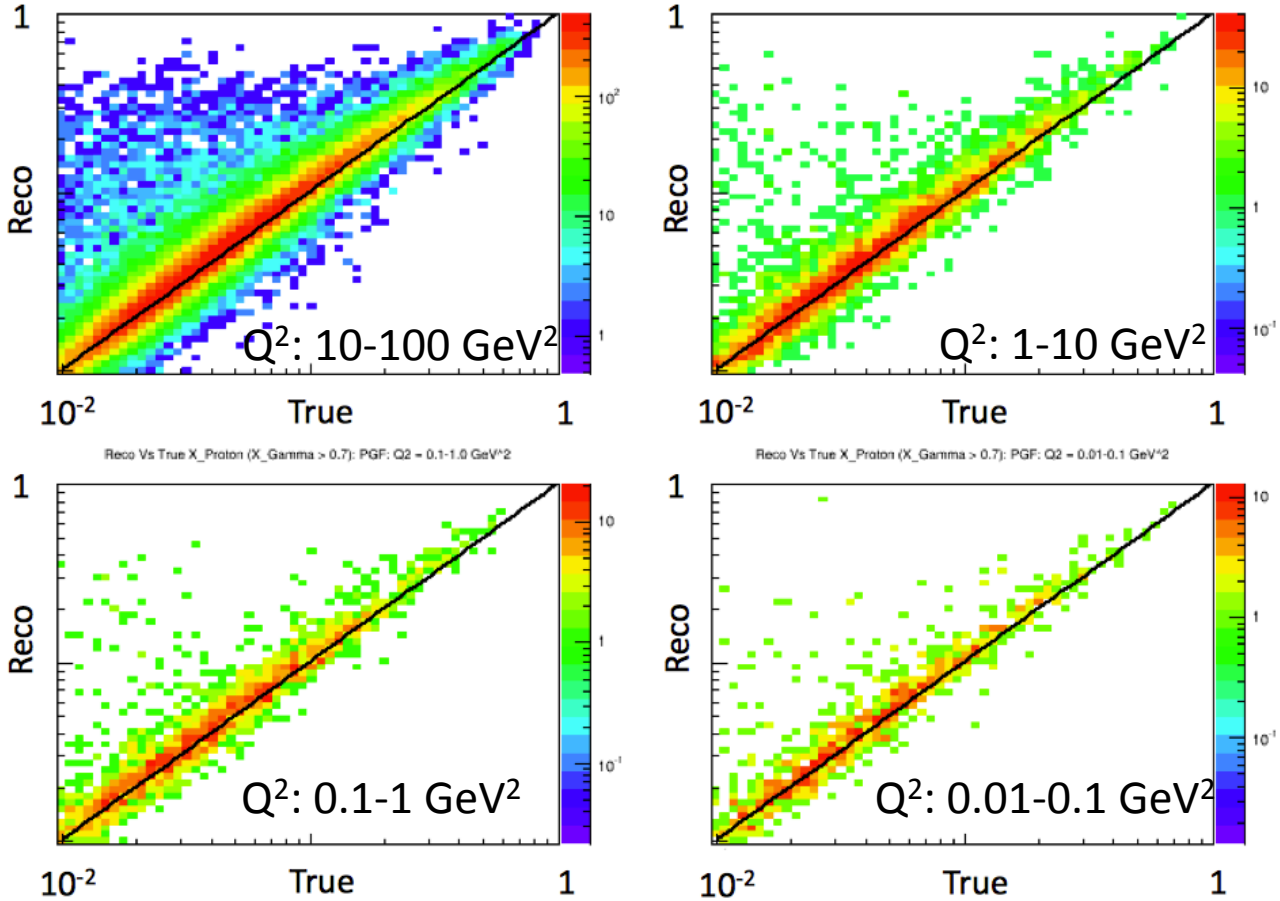

$$x_p^{rec} = \frac{1}{2E_p}(p_{T1}e^{\eta_1} + p_{T2}e^{\eta_2})$$

- To measure gluon, need to probe the parton coming from the proton
- Momentum fraction of the parton from proton is well reconstructed

Polarized photon PDFs

Based on the unpolarized data from PYTHIA, we add a weight on an event-by-event basis just in analysis code to make it polarized.

- In resolved process, For each event, ab $\longrightarrow$ cd process, the weight is calculated as:

$$w = \hat{a}(\hat{s},\hat{t},\mu^2,Q^2) \bullet \frac{\Delta f_a^{\gamma^*}(x_a,\mu^2)}{f_a^{\gamma^*}(x_a,\mu^2)} \bullet \frac{\Delta f_b^{N}(x_b,\mu^2)}{f_b^{N}(x_b,\mu^2)}$$

the input pol photon and proton PDFs, we can get **delta_f**

$$\hat{a}(\hat{s},\hat{t},\mu^2) = \Delta\hat{\sigma}/(2\hat{\sigma})$$

Hard subprocess asymmetry depending on the type of the 2-2 process, the parton kinematics described by Mandelstam variables and photon virtuality.

Unplo photon PDFs and **Unpol proton PDFs,** from **LHAPDF** to get the unpol photon PDFs

Histogram ->Fill(variable, weight)

Hard process Asymmetry $\hat{a}$

$$w = \boxed{\hat{a}(\hat{s},\hat{t},\mu^2,Q^2)} \bullet \frac{\Delta f_a^{\gamma^*}(x_a,\mu^2)}{f_a^{\gamma^*}(x_a,\mu^2)} \bullet \frac{\Delta f_b^N(x_b,\mu^2)}{f_b^N(x_b,\mu^2)}$$

Reaction	$d\hat{\sigma}/d\hat{t}$	$d\Delta\hat{\sigma}/d\hat{t}$
$qg \to qg$	$(\hat{s}^2+\hat{u}^2)[\frac{1}{\hat{t}^2}-\frac{4}{9\hat{s}\hat{u}}]$	$2(\hat{u}^2-\hat{s}^2)[\frac{4}{9\hat{s}\hat{u}}-\frac{1}{\hat{t}^2}]$
$\bar{q}g \to \bar{q}g$	$(\hat{s}^2+\hat{u}^2)[\frac{1}{\hat{t}^2}-\frac{4}{9\hat{s}\hat{u}}]$	$2(\hat{u}^2-\hat{s}^2)[\frac{4}{9\hat{u}\hat{s}}-\frac{1}{\hat{t}^2}]$
$gg \to q\bar{q}$	$\frac{\hat{u}^2+\hat{t}^2}{6\hat{u}\hat{t}}-\frac{3}{8}\frac{\hat{t}^2+\hat{u}^2}{\hat{s}^2}$	$\frac{3}{4}\frac{\hat{t}^2+\hat{u}^2}{\hat{s}^2}-\frac{\hat{u}^2+\hat{t}^2}{3\hat{u}\hat{t}}$
$gg \to gg$	$\frac{9}{2}(3-\frac{\hat{t}\hat{u}}{\hat{s}^2}-\frac{\hat{s}\hat{u}}{\hat{t}^2}-\frac{\hat{s}\hat{t}}{\hat{u}^2})$	$9(-3+2\frac{\hat{s}^2}{\hat{u}\hat{t}}+\frac{\hat{u}\hat{t}}{\hat{s}^2})$
$q_aq_b \to q_aq_b$	$\frac{4}{9}[\frac{\hat{s}^2+\hat{u}^2}{\hat{t}^2}+\delta_{ab}(\frac{\hat{s}^2+\hat{t}^2}{\hat{u}^2}-\frac{2\hat{s}^2}{3\hat{t}\hat{u}})]$	$\frac{8}{9}[\frac{\hat{s}^2-\hat{u}^2}{\hat{t}^2}-\delta_{ab}(\frac{\hat{t}^2-\hat{s}^2}{\hat{u}^2}+\frac{2\hat{s}^2}{3\hat{t}\hat{u}})]$
$q_a\bar{q}_b \to q_c\bar{q}_d$	$\frac{4}{9}[\delta_{ac}\delta_{bd}\frac{\hat{u}^2}{\hat{t}^2}+\delta_{cd}\delta_{ab}\frac{\hat{t}^2+\hat{u}^2}{\hat{s}^2}-\delta_{ad}\delta_{cd}\frac{2\hat{u}^2}{3\hat{s}\hat{t}}+\delta_{ab}\delta_{bd}\frac{\hat{s}^2}{\hat{t}^2}]$	$\frac{8}{9}[-\delta_{ac}\delta_{bd}\frac{\hat{u}^2}{\hat{t}^2}-\delta_{cd}\delta_{ab}\frac{\hat{t}^2+\hat{u}^2}{\hat{s}^2}+\delta_{ad}\delta_{cd}\frac{2\hat{u}^2}{3\hat{s}\hat{t}}+\delta_{ab}\delta_{bd}\frac{\hat{s}^2}{\hat{t}^2}]$
$q\bar{q} \to gg$	$\frac{32}{27}\frac{\hat{t}^2+\hat{u}^2}{\hat{u}\hat{t}}-\frac{8}{3}\frac{\hat{t}^2+\hat{u}^2}{\hat{s}^2}$	$-\frac{64}{27}\frac{\hat{t}^2+\hat{u}^2}{\hat{u}\hat{t}}+\frac{16}{3}\frac{\hat{t}^2+\hat{u}^2}{\hat{s}^2}$

[ref: 10.1007/JHEP08(2010)130]

$$\hat{a}(\hat{s},\hat{t},\mu^2) = \Delta\hat{\sigma}/(2\hat{\sigma})$$

$$\hat{s} = (p_a+p_b)^2, \hat{t} = (p_a-p_c)^2, \hat{u} = (p_a-p_d)^2$$

$\frac{\Delta f_a^{\gamma^*}(x_a,\mu^2)}{f_a^{\gamma^*}(x_a,\mu^2)}$ Depending on flavor

$$w = \hat{a}(\hat{s},\hat{t},\mu^2,Q^2) \bullet \boxed{\frac{\Delta f_a^{\gamma^*}(x_a,\mu^2)}{f_a^{\gamma^*}(x_a,\mu^2)}} \bullet \frac{\Delta f_b^{N}(x_b,\mu^2)}{f_b^{N}(x_b,\mu^2)}$$

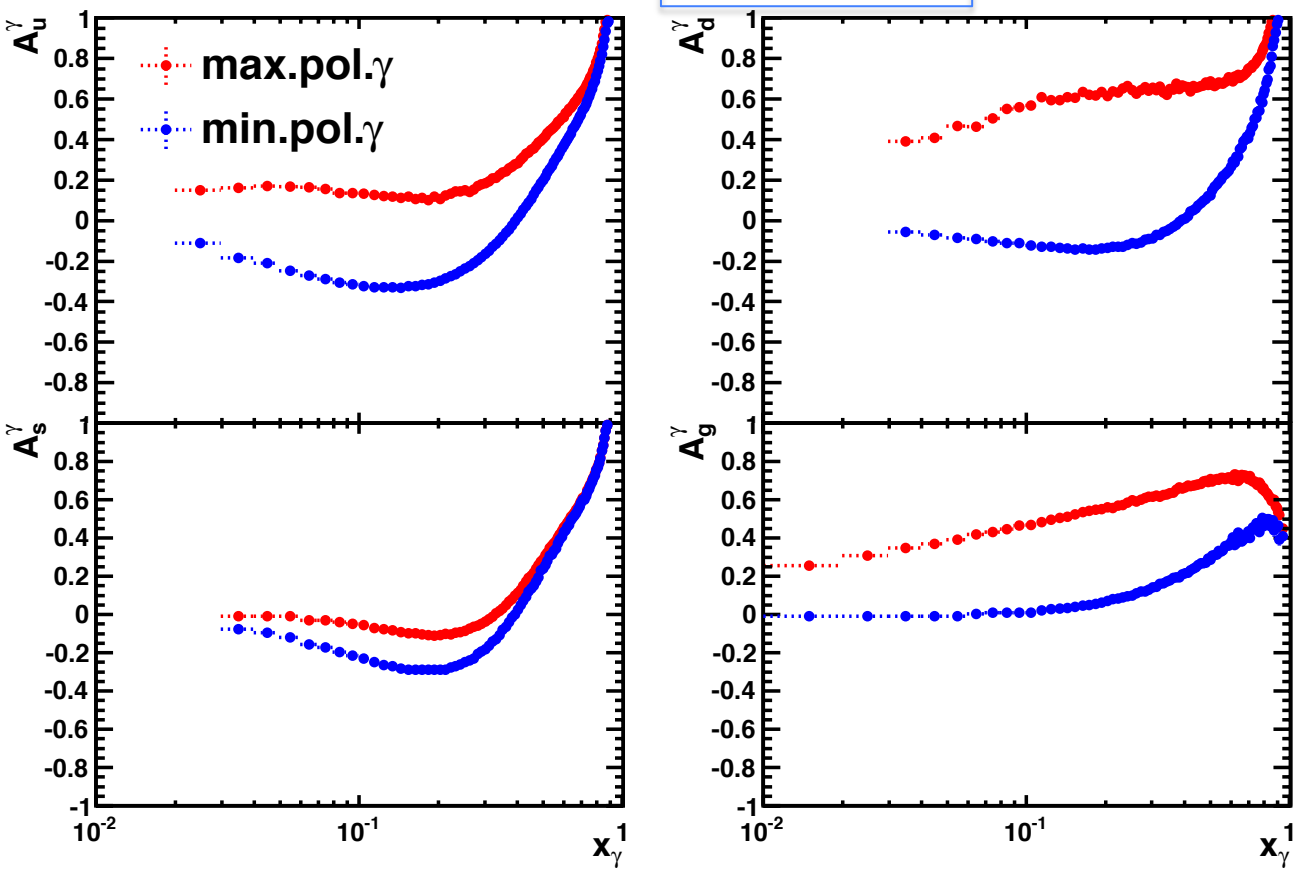

[ref: Z. Phys. C55 (1992) 353; C57 (1993) 309; Phys. Lett. B337 (1994) 373;Phys. Lett. B386 (1996) 370]

$\frac{\Delta f_a^{\gamma^*}(x_a,\mu^2)}{f_a^{\gamma^*}(x_a,\mu^2)}$ Depending on flavor

$$w = \hat{a}(\hat{s},\hat{t},\mu^2,Q^2) \bullet \frac{\Delta f_a^{\gamma^*}(x_a,\mu^2)}{f_a^{\gamma^*}(x_a,\mu^2)} \bullet \boxed{\frac{\Delta f_b^{N}(x_b,\mu^2)}{f_b^{N}(x_b,\mu^2)}}$$

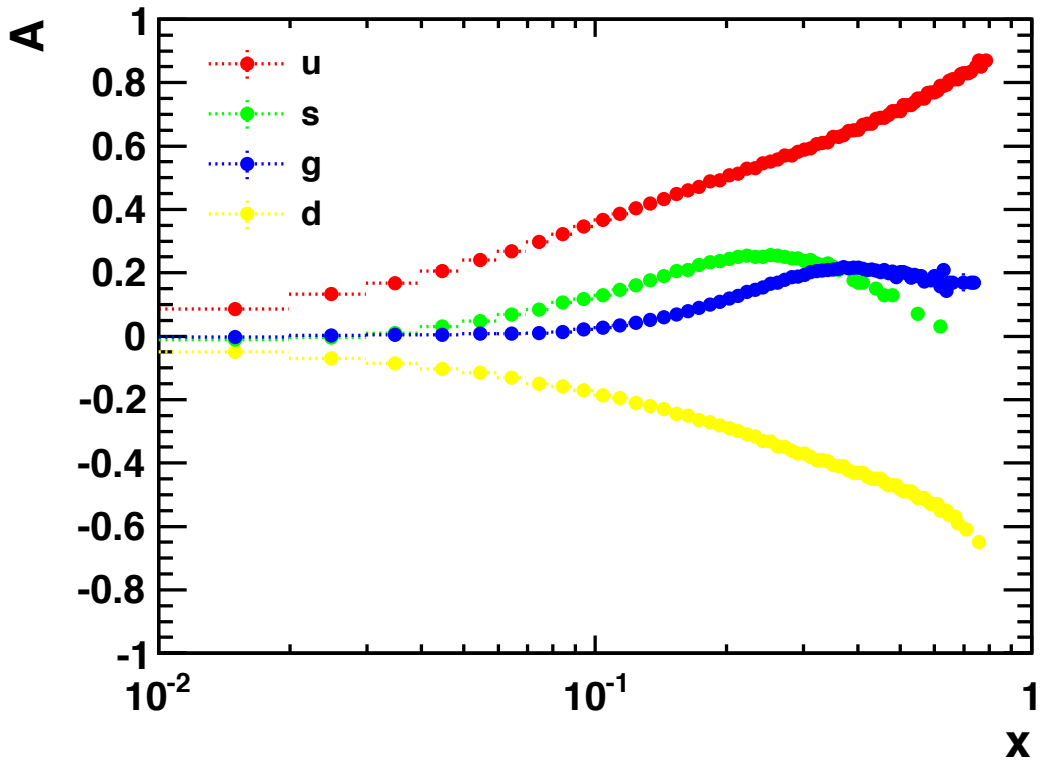

[ref: Phys. Rev. Lett. 101 (2008) 72001; Phys. Rev. D 80 (2009) 034030]

EIC Advantage

- Low Q^2 tagger

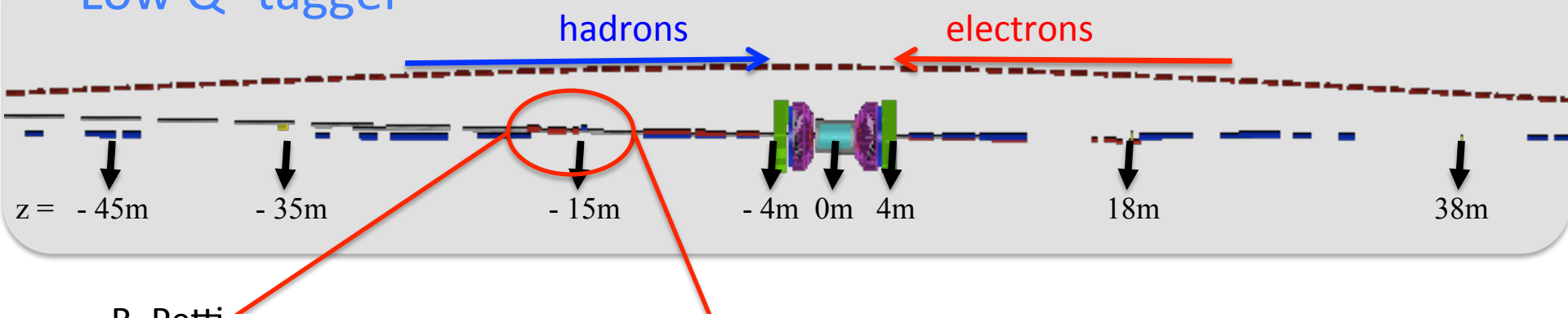

R. Petti

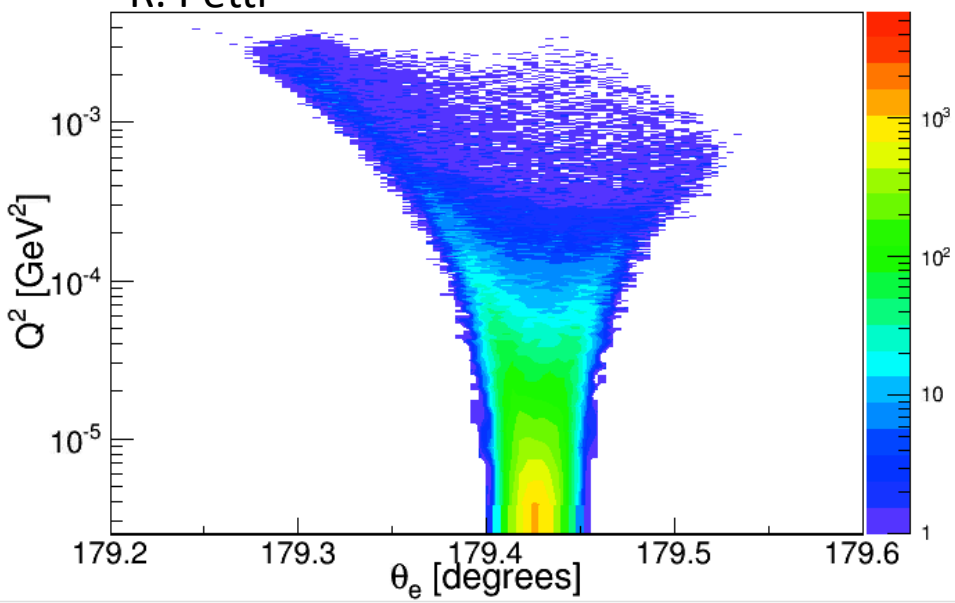

- pythia events with electron reconstructed in the tagger
- acceptance for electrons down to $Q^2 \sim 1\times10^{-5}$ GeV^2
- advantage compared with HERA: tag the outgoing electron directly

How to match di-jet with two final partons

Geometric match:

$$\Delta R\{parton - jet\} = \sqrt{\Delta\phi^2 + \Delta\eta^2}$$

$$\Delta E\{parton - jet\}$$

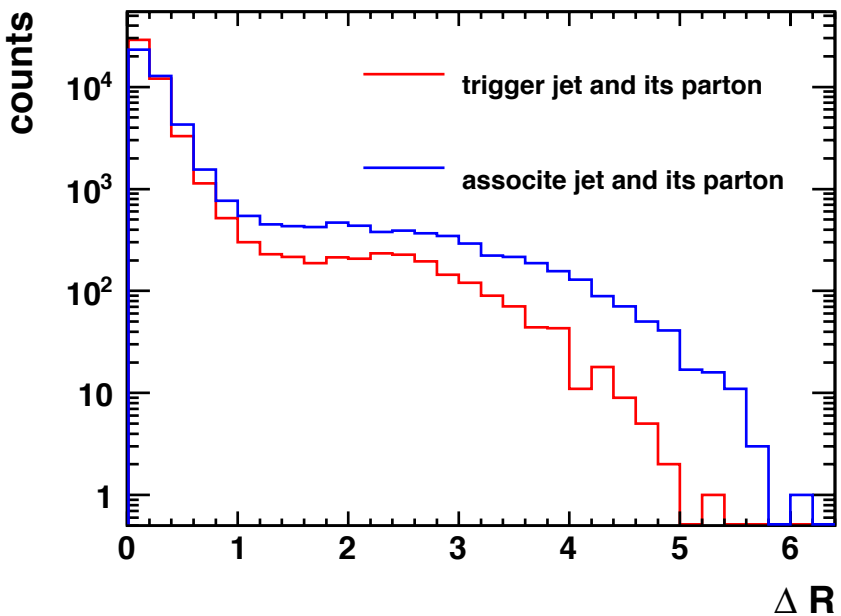

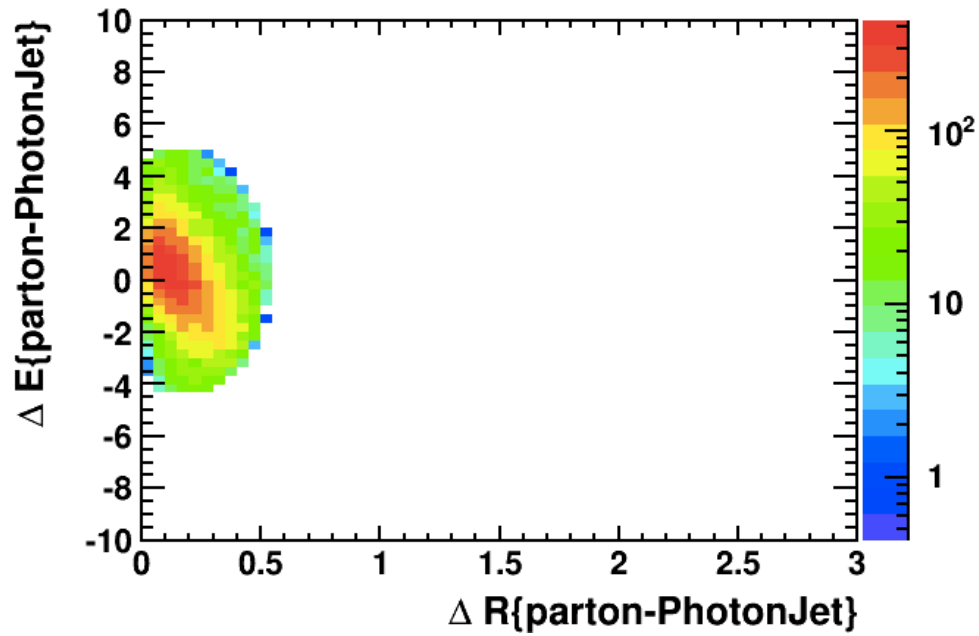

beamparton

tgtparton

→ **Two final partons** → ✓ **match** → **Di-jet**

x^{rec}_{γ} separation

Di-hadron method

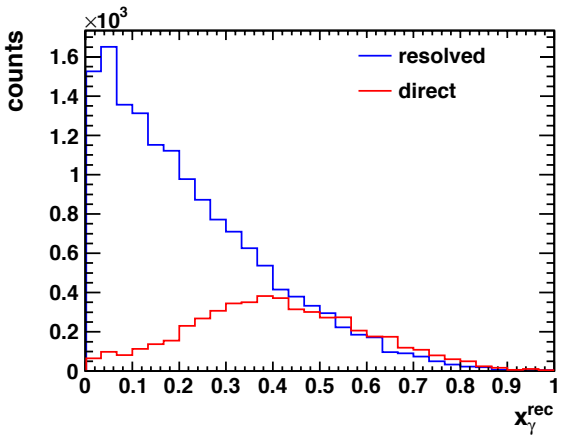

Di-jet method

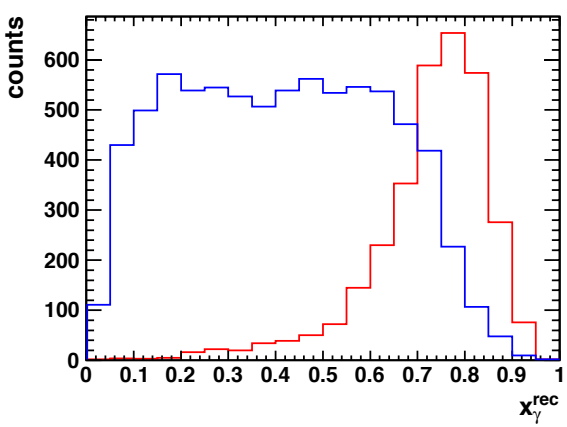

If we choose different x^{rec}_{γ} cut, how well can we separate resolved/direct processes:

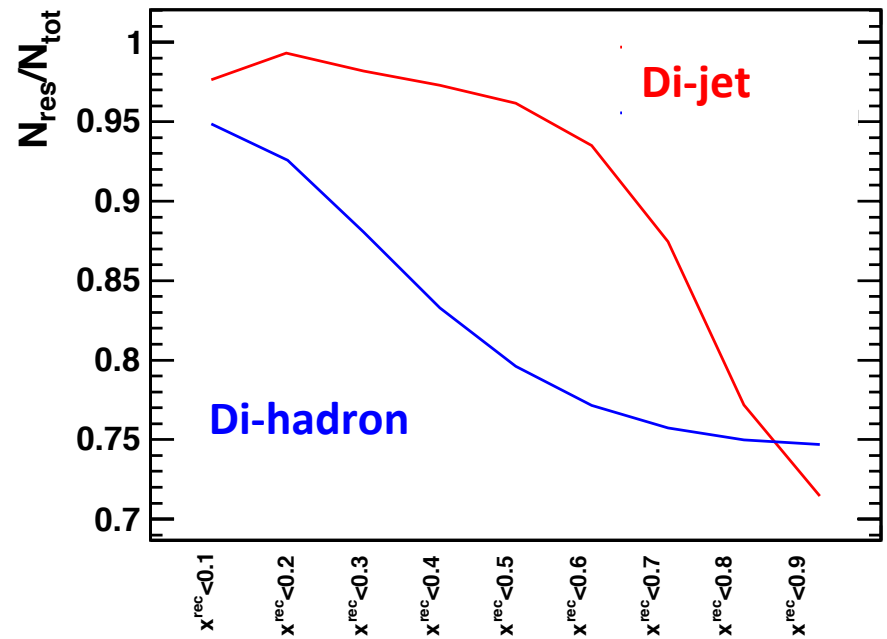

- **Small x^{rec}_{γ}: mainly resolved contribution**
- **Large x^{rec}_{γ}: mainly direct contribution**

- **Di-jet method shows better separation of resolved and direct photon**

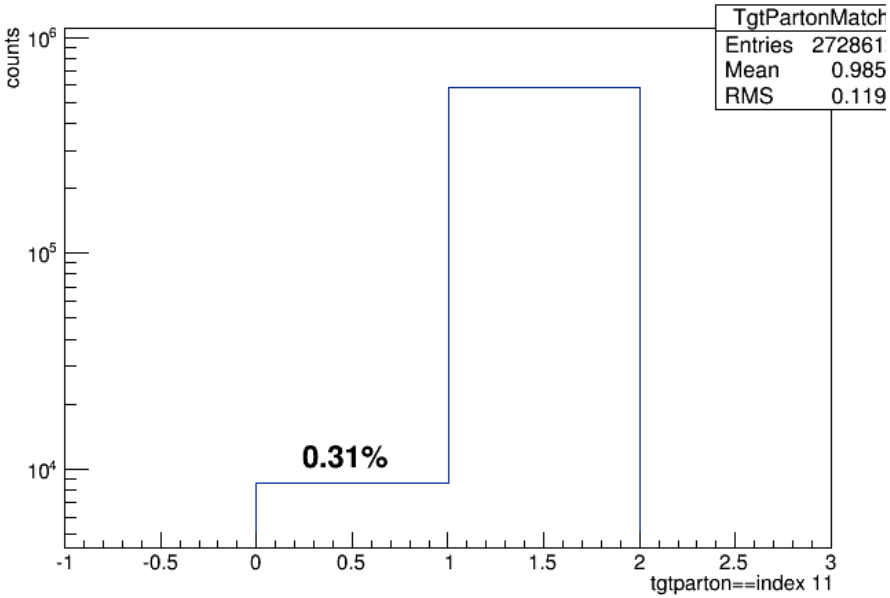

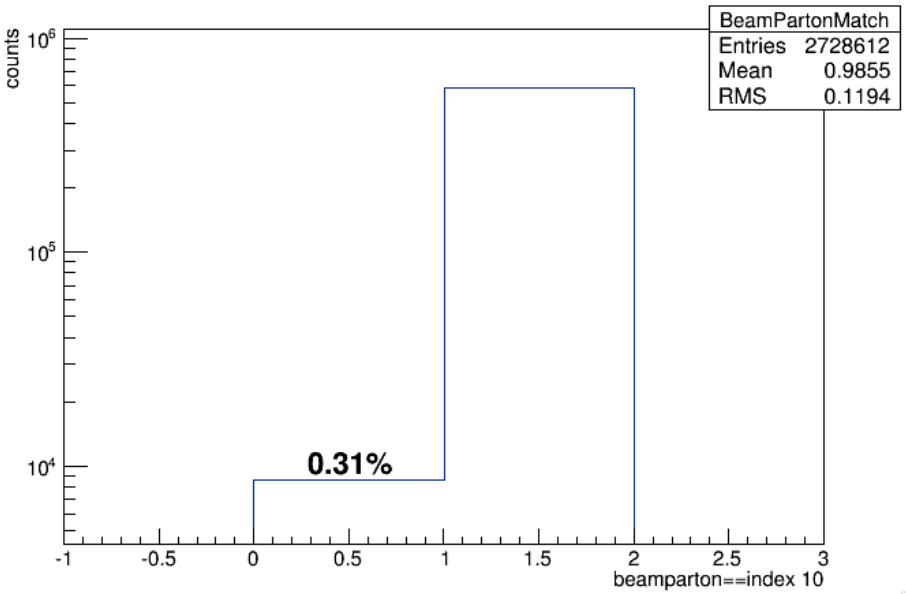

Flavor match: beamparton – index 9
tgtparton – index 10

h_{LAB} separation

Di-hadron method

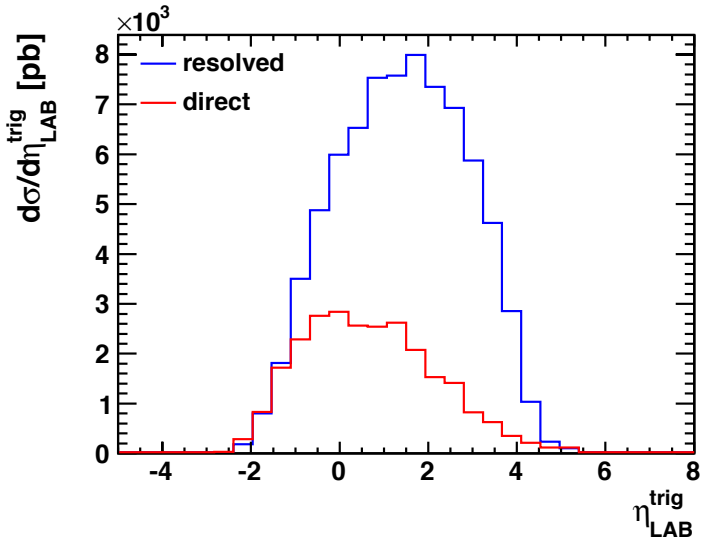

Di-jet method

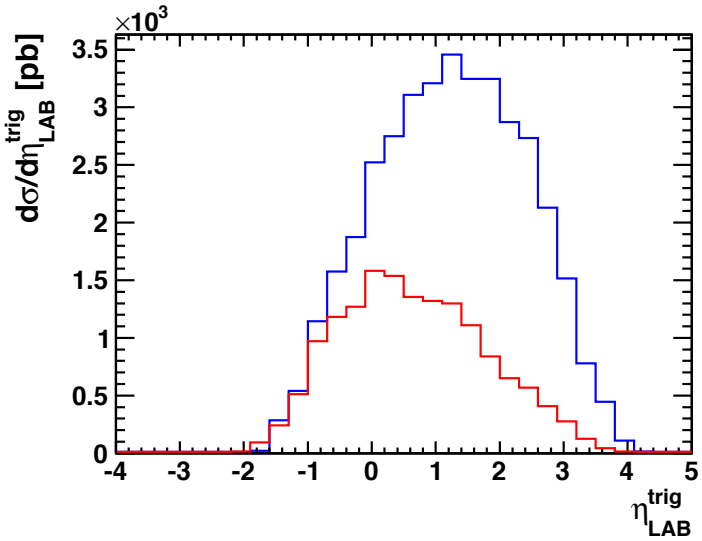

- **For both methods:**
  - **- At positive η_{LAB}, especially $\eta_{LAB} > 2$, the cross section is dominated by resolved process.**

$\eta^{asso}{}_{LAB}$ distribution of associate hadron/jet shows the same results

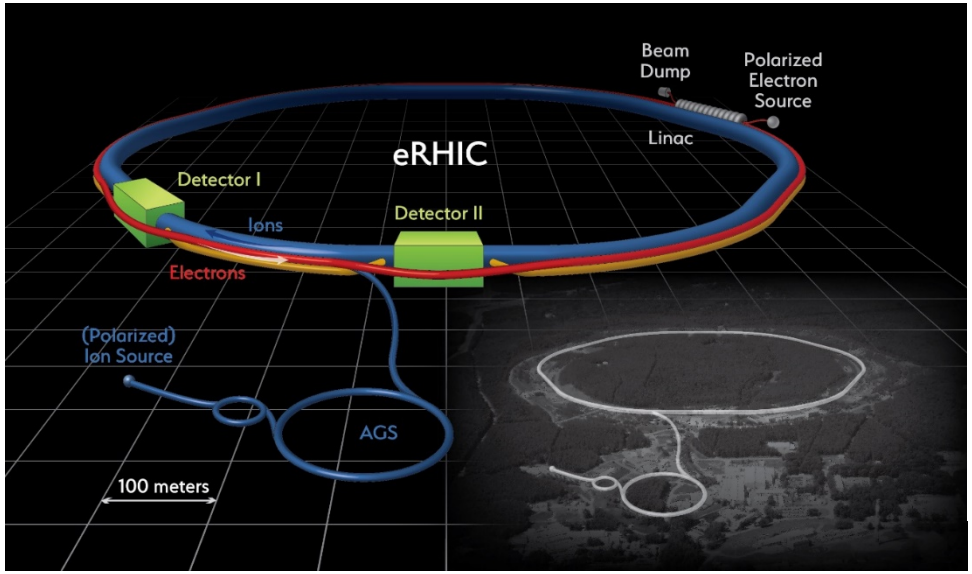
Beam Dump
Polarized Electron Source
Linac
eRHIC
Detector I
Detector II
Ions
Electrons
(Polarized) Ion Source
AGS
100 meters

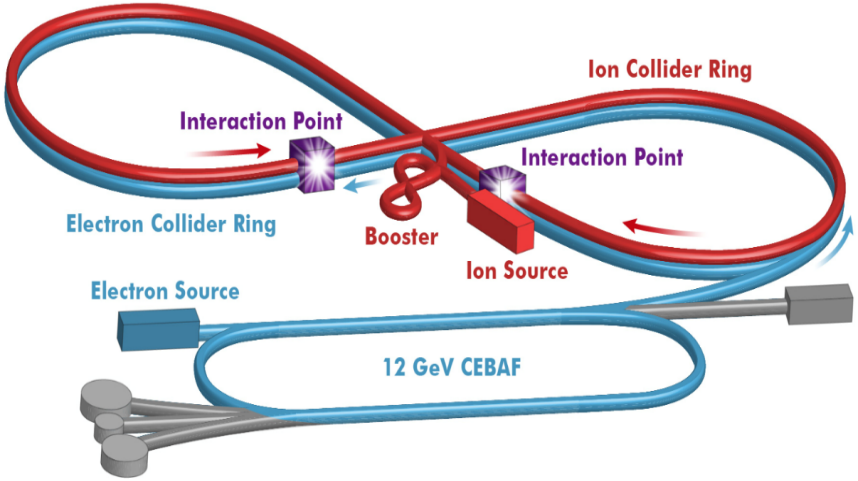
Ion Collider Ring
Interaction Point
Interaction Point
Electron Collider Ring
Booster
Ion Source
Electron Source
12 GeV CEBAF

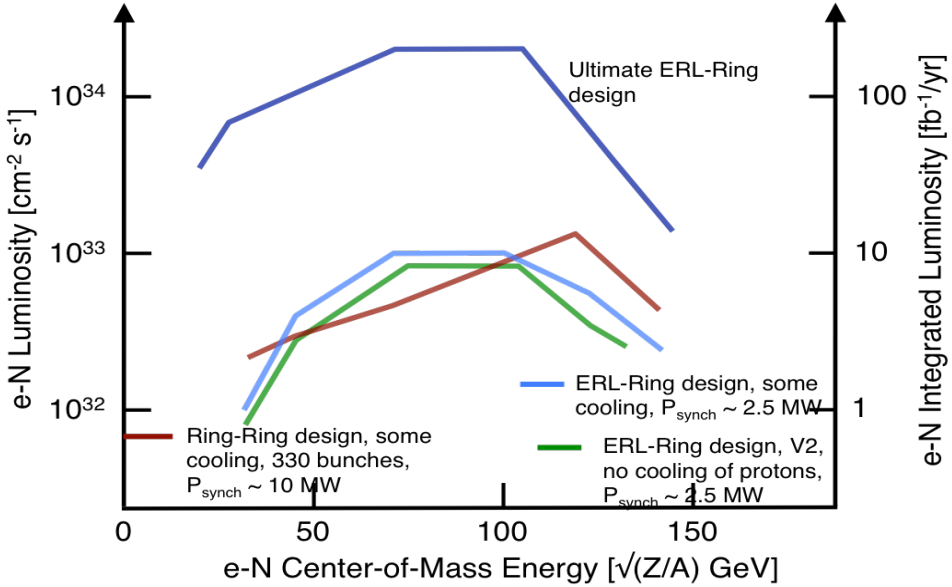
e-N Luminosity [cm^{-2} s^{-1}]
10^{34}
10^{33}
10^{32}
e-N Integrated Luminosity [fb^{-1}/yr]
100
10
1
Ultimate ERL-Ring design
ERL-Ring design, some cooling, P_{synch} ~ 2.5 MW
Ring-Ring design, some cooling, 330 bunches, P_{synch} ~ 10 MW
ERL-Ring design, V2, no cooling of protons, P_{synch} ~ 2.5 MW
0
50
100
150
e-N Center-of-Mass Energy [√(Z/A) GeV]

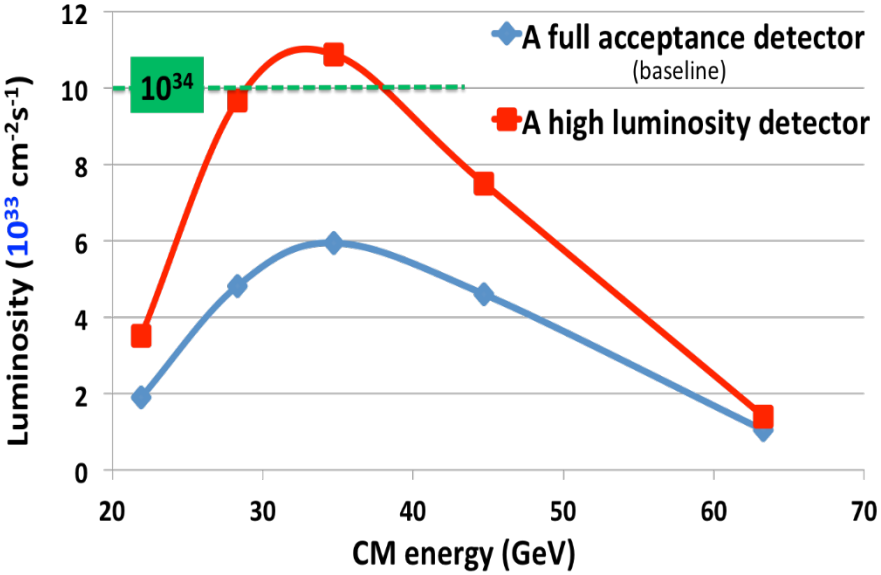
Luminosity (10^{33} cm^{-2}s^{-1})
12
10
8
6
4
2
0
10^{34}
A full acceptance detector (baseline)
A high luminosity detector
20
30
40
50
60
70
CM energy (GeV)

eRHIC arXiv:1409.1633

JLEIC arXiv:1504.07961

Both machine designs built on existing machines

Linac - Ring

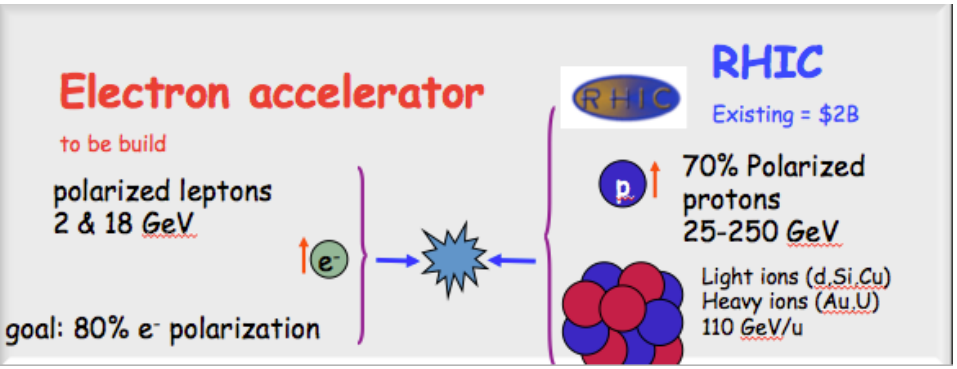

full √s range available from beginning

→ staging in luminosity

Ring- Ring

reuse Cebaf as full energy lepton injector

electron: 3-10 GeV

protons: 20-100 GeV

ions: 8-40 GeV/u for Pb

polarised ions: p, d, 3He, possibly Li

Polarisation for both beams: > 70%

Luminosity 10^{33} to 10^{34} $cm^{-2}s^{-1}$

→ staging center-of-mass energy

Both machines utilize crossing angles

10 mrad 50 mrad

→ need for Crab cavities

Bunch frequency: 9.4 MHz

Bunch frequency: 476 MHz

159 MHz@√s=63GeV

Both designs take great care to have maximal to full acceptance for scattered protons from diffractive reactions, breakup neutrons and spectator tagging

2 interaction regions

Introduction of photon structure

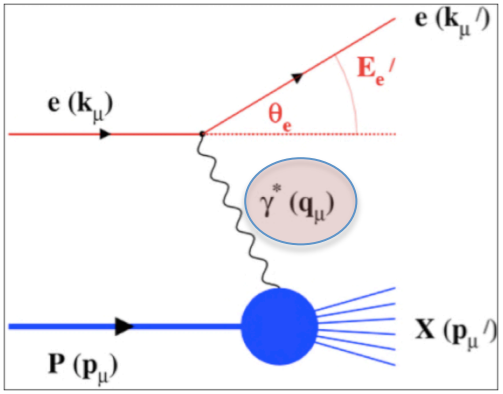

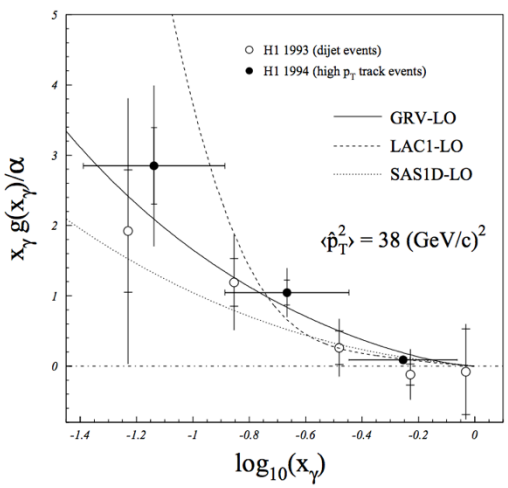

HERA data: gluon density of the photon

- Behavior of the exchanged photon: Bare photon state, **Hadronic photon state**
- Photon can be superposition of above states! ($t \approx E / M^2$)
- The "internal structure" of photons is a manifestation of **quantum fluctuations:** Photon splits into parton content
- We measure the photon structure in **photoproduction:** Low Q^2 events
- **Photon Parton Distribution Functions(PDFs):** Density of the partons

$$f(x,Q^2) \left\{ \begin{array}{l} q(x,Q^2) \\ \bar{q}(x,Q^2) \\ g(x,Q^2) \end{array} \right.$$

- **Unpolarized photon structure:**
  arXiv:9504004, arXiv:9710018, Eur. Phys. J. C 10, 363-372 (1999), DESY 97-164
- **Polarized photon structure:** (critical input for ILC γγ option)
  Experiment: no data
  Theory: Z. Phys. C 74, 641—650 (1997) and arXiv:971125

x_γ is defined as the momentum fraction of the parton from the photon

Parton-jet match

In PYTHIA, beamparton, tgtparton

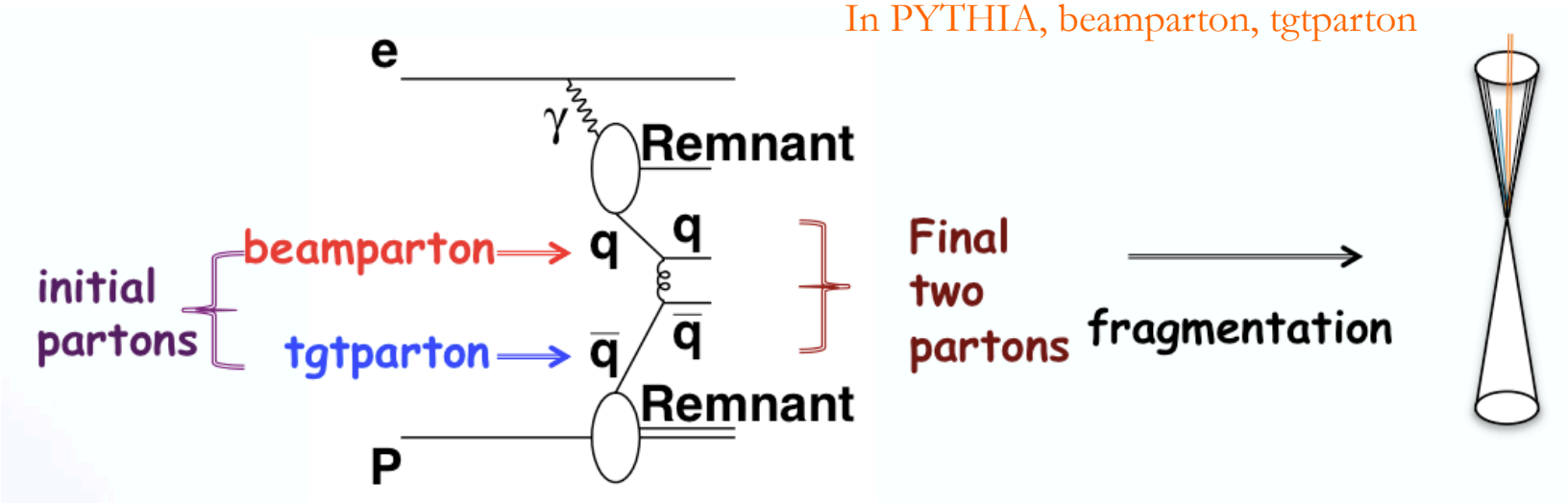

- As we have known how to separate "direct" and "resolved" process, then we measure jet kinematics in resolved process
- Basic info about resolved process and how to tag di-jet back to two final partons
- "Path" to do parton-jet match:
  - beamparton - one final parton - one jet of di-jet ⟹ Jet from photon side
  - tgtparton - another final parton - another jet of di-jet ⟹ Jet from proton side
- Geometric match $\Delta R\{parton - jet\} = \sqrt{\Delta\phi^2 + \Delta y^2}$
  $\Delta E\{parton - jet\}$

Tagging gluon jet

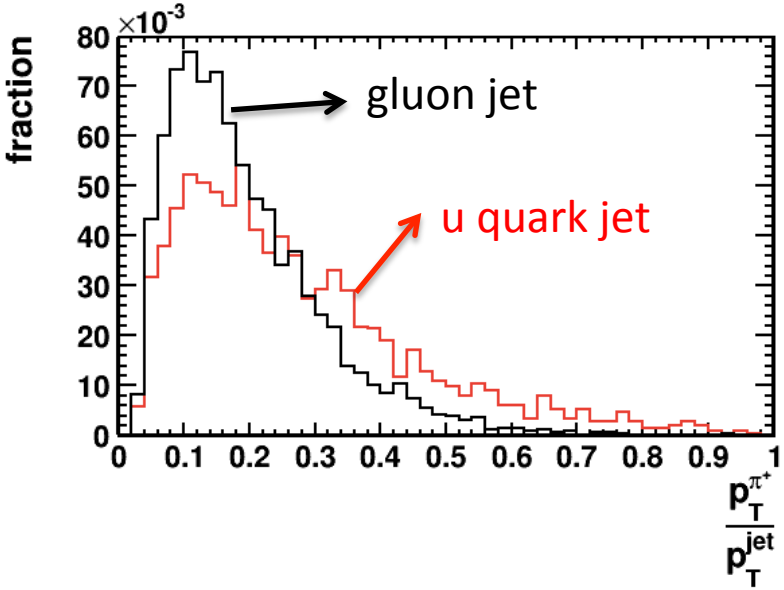

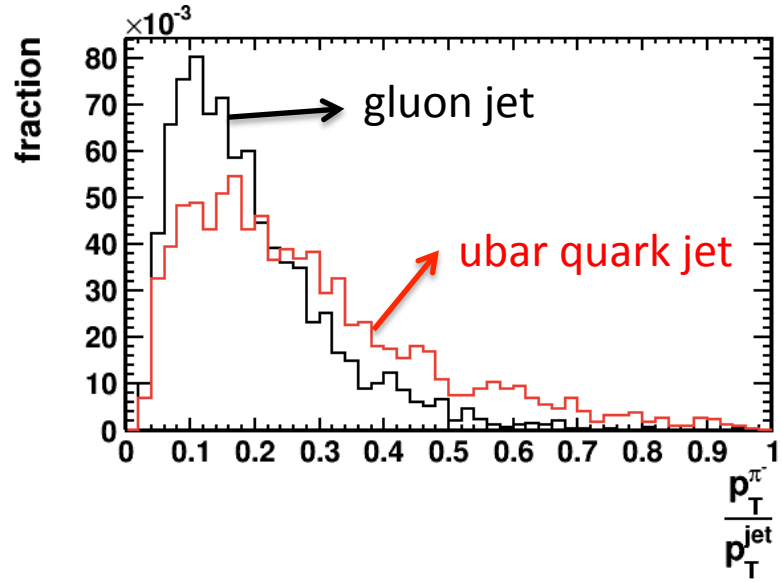

Leading Pion (the highest pt pion) pt fraction compared to the jet pt

- Leading pion plots show better sensitivity
- It's easy to identify quark jet, but not for gluon jet